J. Math. Anal. Appl. 362 (2010) 252–274

Contents lists available at ScienceDirect

Journal of Mathematical Analysis and Applications

www.elsevier.com/locate/jmaa

Chaos control and chaos synchronization for multi-scroll chaotic attractors generated using hyperbolic functions

F. Xu, Pei Yu *

Department of Applied Mathematics, The University of Western Ontario, London, Ontario, N6A 5B7, Canada

ARTICLE INFO

Article history:
Received 26 September 2008
Available online 18 March 2009
Submitted by Goong Chen

Keywords:
Multi-scroll chaotic attractors
Hyperbolic tangent function
Feedback control
Lyapunov function
Global and exponential stabilization
Global and exponential synchronization

ABSTRACT

In this paper, we design a series of chaotic systems that can generate one-directional, two-directional and three-directional multi-scroll chaotic attractors. Then, based upon the properties of these chaotic systems, we construct appropriate Lyapunov functions and design simple linear feedback controls to globally exponentially stabilize and synchronize these chaotic systems. Numerical simulation results are also presented to show the applicability of the proposed control laws.

1. Introduction

The study on multi-scroll chaotic attractors has received increasing attention over the past few decades. The first multi-scroll chaotic attractor can be traced back to Chua's circuit [1], which displays a double-scroll chaotic attractor. Later, one-directional n-scroll chaotic attractors were developed [2–9]. Recently the research on multi-scroll chaotic systems was extended to the study of two-directional and three-directional chaotic attractors [10–12]. Meanwhile, piecewise linear functions played an important part in the designing of multi-scroll chaotic attractors. Chua's circuit used piecewise linear function as the non-linear term [1]. Recent research shows that simple piecewise linear function could be extended to the multilevel piecewise linear function to generate multi-directional, multi-scroll chaotic attractors [11].

Chaos control and chaos synchronization play a very important role in the study of chaotic systems and have great significance in the application of chaos. Since chaos is very sensitive to its initial condition, chaos control and chaos synchronization were once believed to be impossible. However, two important discoveries completely changed this situation. One of them is the OGY method [13] developed in the 1990's. The other is the concept of chaos synchronization proposed by Pecora and Garrol [14] in 1990. Up to now, the study of chaos control and chaos synchronization was mostly focused on classical chaotic systems such as the Lorenz system, Chua circuit, Chen system, Lü system etc. (e.g., see [21–27]). Very few results have been obtained for chaos control and chaos synchronization of more complicated multi-directional multi-scroll chaotic attractors.

In this paper, other than applying the traditionally widely used piecewise linear functions, we use hyperbolic function series in a simple linear system to generate a series of one-directional, two-directional and three-directional multi-scroll chaotic attractors. The hyperbolic function, as a continuously differentiable function, is easier to analyze chaos control and chaos synchronization. On the other hand, since hyperbolic tangent function is frequently used to characterize the behavior

* Corresponding author. Fax: +1 519 661 3523.
E-mail address: pyu@pyu1.apmaths.uwo.ca (P. Yu).

0022-247X/$ – see front matter
doi:10.1016/j.jmaa.2009.03.041

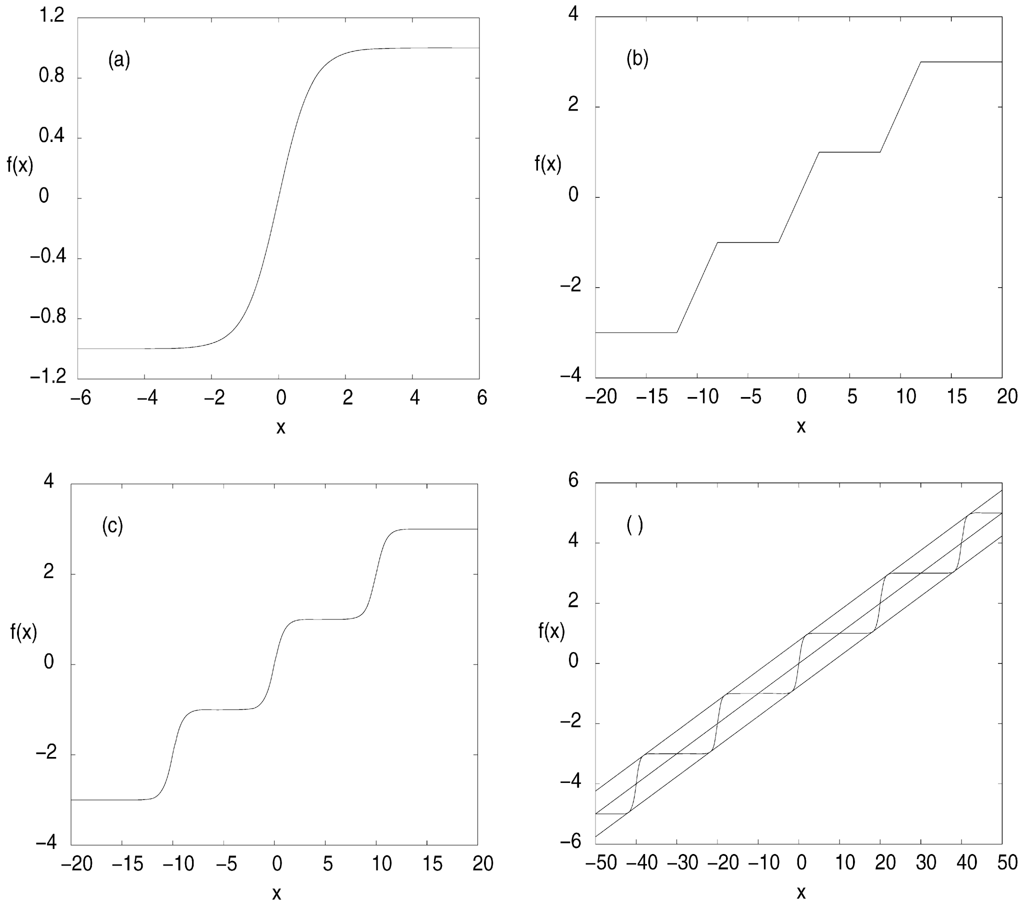

Fig. 1. (a) Sigmoidal hyperbolic function $f(x) = \tanh(x)$; (b) piecewise linear "stair" function; (c) hyperbolic tangent function series $f(x) = \sum_{j=-1}^{1} \tanh(x + j\tau)$ with $\tau = 10$; and (d) hyperbolic tangent function series $f(x) = \sum_{j=-2}^{2} \tanh(x + j\tau)$ with $\tau = 20$, showing the "envelop" tangent lines to the graph, and the number of intersection points of the line $y = \frac{2}{\tau}x$ with the graph being $4 \times 2 + 3 = 11$.

of neural networks, such a study may help understand complex dynamical behavior existing in neural networks. Then, based on the properties of the chaotic system, we design simple feedback controls to globally exponentially stabilize and synchronize the chaotic systems. Corresponding Lyapunov functions were presented and used to prove the proposed control laws. Then numerical simulation examples were showed to verify the applicability of the control laws.

The rest of the paper is organized as follows. In Section 2, the hyperbolic tangent function and hyperbolic tangent function series are defined. Then 1-D-n-scroll, 2-D-$m \times n$-grid-scroll, 3-D-$m \times n \times l$-grid-scroll chaotic attractors are obtained in Sections 3, 4 and 5, respectively. Chaos control and chaos synchronization for 1-D-n-scroll, 2-D-$m \times n$-grid-scroll and 3-D-$m \times n \times l$-grid-scroll chaotic attractors are studied in Sections 6, 7 and 8, respectively. Conclusion is given Section 9.

2. Definition of hyperbolic tangent function series

The hyperbolic tangent function is described by the following equation:

$$f(x) = \tanh x = \frac{\sinh x}{\cosh x} = \frac{e^x - e^{-x}}{e^x + e^{-x}} \tag{1}$$

which, as shown in Fig. 1(a), is monotone increasing for $-\infty < x < \infty$ and bounded, $-1 < \tanh(x) < 1$. This is a typical characteristic function in describing many neural networks [15], which can be replaced by piecewise linear functions (see Fig. 1(b)) particularly used in circuits design. Recently, multilevel piecewise linear functions have been used in CNNs [15]. This multilevel piecewise linear function may be replaced by an infinitely differentiable function, described by the following so-called *hyperbolic tangent function series*:

$$F(x) = \sum_{j=-r}^{s} \tanh(x + j\tau), \tag{2}$$

where the parameter τ is a positive real value, while the parameters r and s are non-negative integers. The function $F(x)$ is depicted in Fig. 1(c), indicating that this function smooths the multilevel piecewise linear function (shown in Fig. 1(b)).

The basic idea in generating multi-scroll chaotic attractors is to add the above hyperbolic tangent function series to a linear system, given by [11]

$$\begin{aligned}
\dot{x} &= y,\\
\dot{y} &= z,\\
\dot{z} &= -ax - by - cz,
\end{aligned} \tag{3}$$

where a, b and c are constant parameters. It is easy to see that the unique equilibrium point of the linear system (3) is the origin $(x, y, z) = (0, 0, 0)$. A linear analysis shows that when

$$a > 0, \qquad c > 0, \qquad bc > a,$$

the equilibrium point is asymptotically stable.

3. Design of 1-D-*n*-scroll chaotic attractors

Based on (3), our proposed model for 1-D chaos generator is given as follows:

$$\begin{aligned}
\dot{x} &= y,\\
\dot{y} &= z,\\
\dot{z} &= -ax - by - cz + a\frac{\tau}{2}\left[(r-s) + \sum_{j=-r}^{s} \tanh(x + j\tau)\right],
\end{aligned} \tag{4}$$

where a, b, c and τ are positive real values, while s and r take non-negative integers, determining the maximum number of chaotic scrolls.

For example, when $a = b = c = 0.65$, $\tau = 100$, and $s = r = 0$, a double-scroll chaotic attractor can be obtained, as shown in Fig. 2(a) and (b). The time history for the x component is depicted in Fig. 2(c). The double-scroll chaotic system (4) has three equilibrium points, $S_0 = (0, 0, 0)$ and $S_{1,2} = (\pm 50, 0, 0)$. The eigenvalues associated with the equilibrium point S_0 are $\lambda_1 = 2.9036$ and $\lambda_{2,3} = -1.7768 \pm 2.7949i$, indicating that S_0 is a saddle point of index one since the real part of the conjugate eigenvalues is negative. The eigenvalues associated with the equilibrium points $S_{1,2}$ are $\lambda_1 = -0.8217$ and $\lambda_{2,3} = 0.0858 \pm 0.8853i$, implying that $S_{1,2}$ are saddle points of index two since the real part of the conjugate eigenvalues is positive. It is known that only equilibria of saddle point of index two can generate scrolls [16,17]. Therefore, $S_{1,2}$, corresponding to the two equilibria of saddle points of index two, are responsible for the generation of the double scrolls, while S_0, on the other hand, is responsible for the connection of the two chaotic scrolls. Another approach to determine whether a system is chaotic or not is to compute its Lyapunov exponents. If a system has at least one positive Lyapunov exponent, and all the trajectories are ultimately bounded, then the system is chaotic [18]. A chaos is called hyperchaos if the system has two or more positive Lyapunov exponents. For system (4) with the given parameter values, numerical simulation results show that trajectories are bounded for different initial points. Further, a numerical method [19] has been employed to obtain the following three Lyapunov exponents:

$$L_1 = 0.1069, \qquad L_2 = -0.005, \qquad L_3 = -0.7520.$$

Hence, $L_1 > 0$ implies that the system is chaotic. The simulation result of the Lyapunov exponents is shown in Fig. 1(d).

When proper coefficients are chosen, system (4) can have $(r + s + 1)$ saddle points of index one (denoted by Γ_x) and $(r + s + 2)$ saddle points of index two (denoted by Γ_x^*):

$$\begin{aligned}
\Gamma_x &\approx \{s\tau, (s-1)\tau, \ldots, -r\tau\},\\
\Gamma_x^* &\approx \left\{(2s+1)\frac{\tau}{2}, (2s-1)\frac{\tau}{2}, \ldots, -(2r+1)\frac{\tau}{2}\right\},
\end{aligned} \tag{5}$$

where the subscript x denotes the non-zero coordinate of the saddle points. Equilibrium points in set Γ_x^*, which have corresponding eigenvalues $\lambda_1 < 0$ and $\lambda_{2,3} = \xi \pm \eta i$ with $\xi > 0$ and $\eta \neq 0$, are responsible for the generation of the $r + s + 2$ scrolls. Equilibrium points in set Γ_x, which have corresponding eigenvalues $\lambda_1 > 0$ and $\lambda_{2,3} = \xi \pm \eta i$ with $\xi < 0$ and $\eta \neq 0$, are responsible for the connection of the $r + s + 2$ scrolls. Thus, system (4) can generate as many as $r + s + 2$ chaotic scrolls. For example, when $a = b = c = 0.65$, $\tau = 100$, $s = r = 3$, the corresponding hyperbolic tangent function series can produce 8-scroll chaotic attractors, see Fig. 3(a) and (b), and the time history for the x component is shown in Fig. 3(c).

The equilibrium points and their corresponding eigenvalues are listed in Table 1. It is seen from the table that the equilibrium points of type two, $S_{7,8}, S_{9,10}, S_{11,12}, S_{13,14}$, are responsible for the generation of the 8 scrolls, while the equilibrium

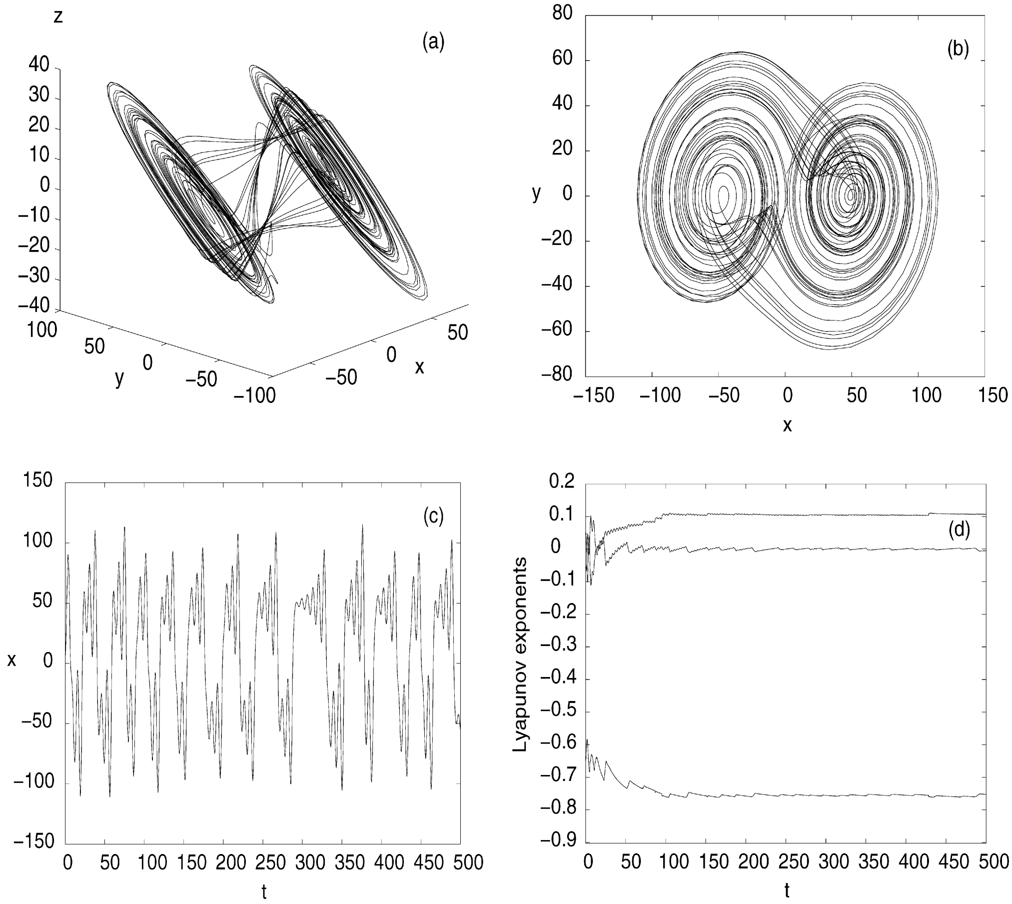

Fig. 2. Simulated results for a double-scroll chaotic attractor of system (4) with $a = b = c = 0.65$, $\tau = 100$, $r = s = 0$: (a) the phase portrait in the x–y–z plane; (b) the phase portrait projected on the x–y plane; (c) the time history $x(t)$; and (d) the Lyapunov exponents.

points of type one, $S_0, S_{1,2}, S_{3,4}, S_{5,6}$, are responsible for the connection of the 8 scroll chaotic attractors. The Lyapunov exponents are found to be

$$L_1 = 0.1337, \qquad L_2 = -0.004, \qquad L_3 = -0.7799,$$

showing that the system is chaotic. The numerical computation result of these Lyapunov exponents is shown in Fig. 3(d).

4. Design of 2-D-$m \times n$-grid-scroll chaotic attractors

The 2-D multi-scroll chaotic attractors can be obtained by adding two hyperbolic tangent function series to system (3) to obtain the following system:

$$\begin{aligned}
\dot{x} &= y - \frac{\tau_2}{2}\left[(r_2 - s_2) + \sum_{j=-r_2}^{s_2} \tanh(y + j\tau_2)\right], \\
\dot{y} &= z, \\
\dot{z} &= -ax - by - cz + a\frac{\tau_1}{2}\left[(r_1 - s_1) + \sum_{j=-r_1}^{s_1} \tanh(x + j\tau_1)\right] + b\frac{\tau_2}{2}\left[(r_2 - s_2) + \sum_{j=-r_2}^{s_2} \tanh(y + j\tau_2)\right],
\end{aligned} \tag{6}$$

where a, b, c, τ_1 and τ_2 are positive real values, while r_1, r_2, s_1, s_2 are non-negative integers. m and n are determined by

$$\begin{aligned}
m &= r_1 + s_1 + 2, \\
n &= r_2 + s_2 + 2.
\end{aligned} \tag{7}$$

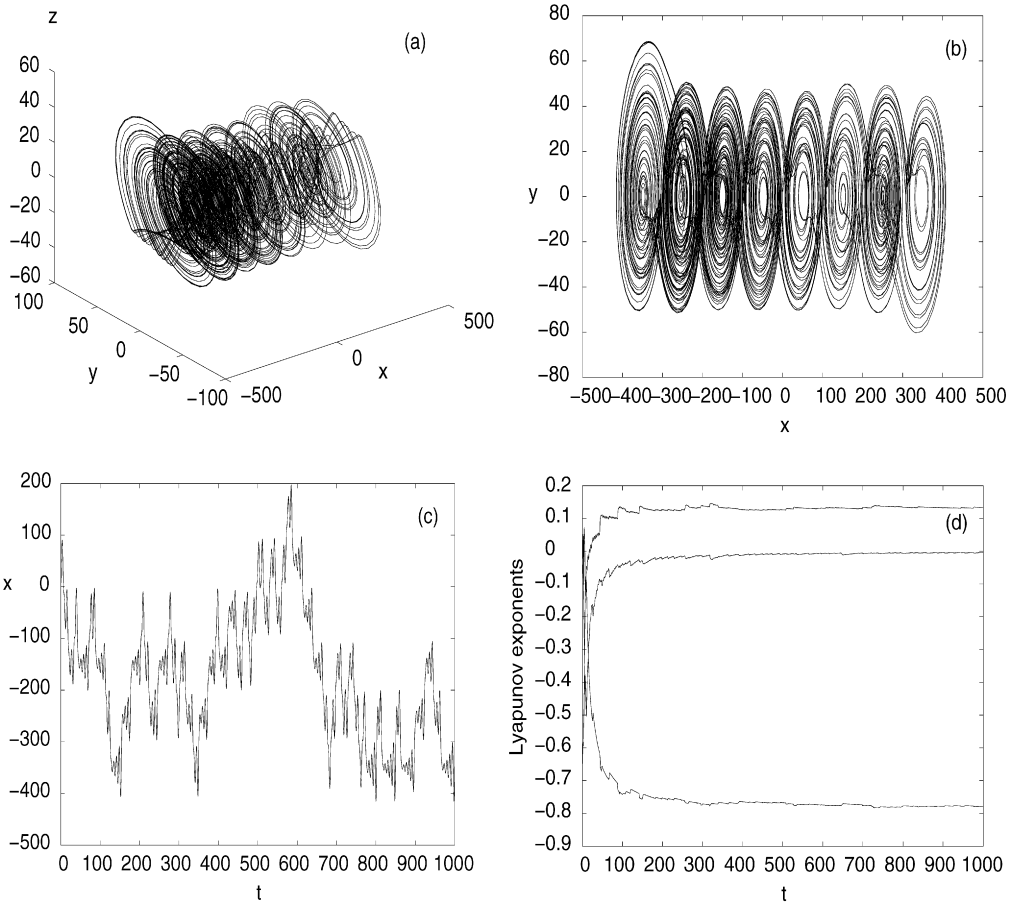

Fig. 3. Simulated results for 1-D 8-scroll chaotic attractor of system (4) with $a = b = c = 0.65$, $\tau = 100$, $r = s = 3$: (a) the phase portrait in the x–y–z plane; (b) the phase portrait projected on the x–y plane; (c) the time history $x(t)$; and (d) the Lyapunov exponents.

Table 1
Equilibrium points and their corresponding eigenvalues for the case of 8 chaotic scrolls (Fig. 3).

Equilibrium points	Corresponding eigenvalues	Type of equilibrium points
S_0 $(0,0,0)$	2.9037, $-1.7768 \pm 2.7949i$	I
$S_{1,2}$ $(\pm 100,0,0)$	2.9037, $-1.7768 \pm 2.7949i$	I
$S_{3,4}$ $(\pm 200,0,0)$	2.9037, $-1.7768 \pm 2.7949i$	I
$S_{5,6}$ $(\pm 300,0,0)$	2.9037, $-1.7768 \pm 2.7949i$	I
$S_{7,8}$ $(\pm 50,0,0)$	-0.8217, $0.0858 \pm 0.8853i$	II
$S_{9,10}$ $(\pm 150,0,0)$	-0.8217, $0.0858 \pm 0.8853i$	II
$S_{11,12}$ $(\pm 250,0,0)$	-0.8217, $0.0858 \pm 0.8853i$	II
$S_{13,14}$ $(\pm 350,0,0)$	-0.8217, $0.0858 \pm 0.8853i$	II

Define

$$\begin{aligned}
&\Gamma_x \approx \{s_1\tau_1, (s_1-1)\tau_1, \ldots, -r_1\tau_1\},\\
&\Gamma_x^* \approx \left\{(2s_1+1)\frac{\tau_1}{2}, (2s_1-1)\frac{\tau_1}{2}, \ldots, -(2r_1+1)\frac{\tau_1}{2}\right\},\\
&\Gamma_y \approx \{s_2\tau_2, (s_2-1)\tau_2, \ldots, -r\tau_2\},\\
&\Gamma_y^* \approx \left\{(2s_2+1)\frac{\tau_2}{2}, (2s_2-1)\frac{\tau_2}{2}, \ldots, -(2r_2+1)\frac{\tau_2}{2}\right\},
\end{aligned} \tag{8}$$

where the subscripts x and y indicate the non-zero coordinates of the saddle points. Then all equilibrium points of system (6) can be classified into the following four different sets:

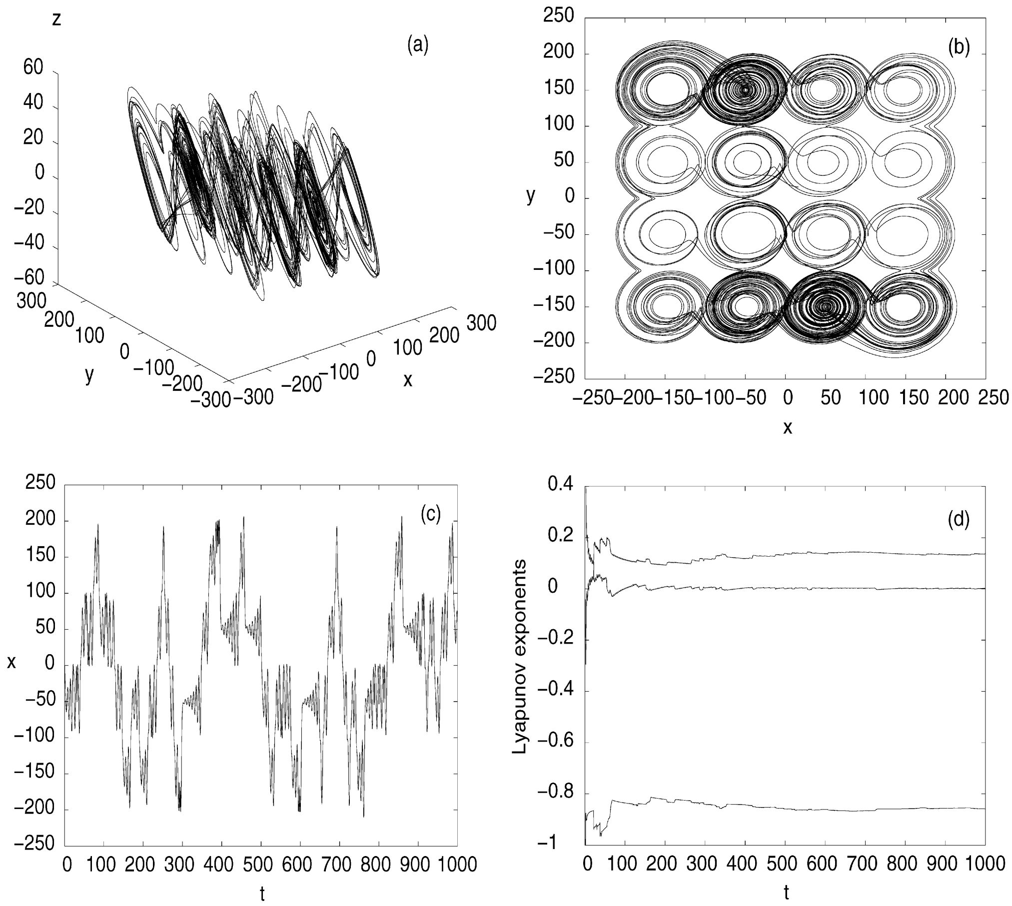

Fig. 4. Simulated results for 2-D 4×4-scroll chaotic attractor of system (6) with $a = b = c = 0.72$, $\tau_1 = \tau_2 = 100$, $r_1 = r_2 = s_1 = s_2 = 1$: (a) the phase portrait in the x–y–z plane; (b) the phase portrait projected on the x–y plane; (c) the time history $x(t)$; and (d) the Lyapunov exponents.

$$\Gamma_1 = \{(x, y) \mid x \in \Gamma_x^*, y \in \Gamma_y^*\},$$
$$\Gamma_2 = \{(x, y) \mid x \in \Gamma_x^*, y \in \Gamma_y\},$$
$$\Gamma_3 = \{(x, y) \mid x \in \Gamma_x, y \in \Gamma_y^*\},$$
$$\Gamma_4 = \{(x, y) \mid x \in \Gamma_x, y \in \Gamma_y\}.$$

A direct calculation shows that only the equilibrium points in set Γ_1 are saddle points of index two with eigenvalues satisfying $\lambda_1 < 0$ and $\lambda_{2,3} = \xi \pm \eta i$ ($\xi > 0$ and $\eta \neq 0$). These equilibrium points are responsible for the generation of $(r_1 + s_1 + 2) \times (r_2 + s_2 + 2)$ chaotic attractors. For example, setting $a = b = c = 0.72$, $\tau_1 = \tau_2 = 100$, and $r_1 = r_2 = s_1 = s_2 = 1$ in system (6), we get a 4×4-grid-scroll chaotic attractors, as shown in Fig. 4(a) and (b).

The three Lyapunov exponents for this system are

$$L_1 = 0.1384, \qquad L_2 = 0, \qquad L_3 = -0.8590,$$

implying that the system is chaotic.

Note that the divergence of system (6) is

$$\nabla V = \frac{\partial \dot{x}}{\partial x} + \frac{\partial \dot{y}}{\partial y} + \frac{\partial \dot{z}}{\partial z} = -c < 0. \tag{9}$$

Hence, the dynamical system described by (6) is dissipative, and an exponential contraction of the system (6) is given by

$$\frac{dV}{dt} = e^{-ct}. \tag{10}$$

Therefore, in dynamical system (6), a volume element V_0 is apparently contracted by the flow into a volume element $V_0 e^{-ct}$ in time t. It means that each volume containing the trajectory of this dynamical system shrinks to zero as $t \to \infty$ at an exponential rate c. So, all the trajectories of this system are eventually confined by a specific subset that has zero volume, and the asymptotic motion settles onto an attractor of system (6).

5. Design of 3-D-$m \times n \times l$-grid-scroll chaotic attractors

Similarly, we may generate 3-D-$m \times n \times l$-grid-scroll chaotic attractors by adding three hyperbolic tangent function series to system (3) to obtain the following system:

$$\begin{aligned}
\dot{x} &= y - \frac{\tau_2}{2}\left[(r_2 - s_2) + \sum_{j=-r_2}^{s_2} \tanh(y + j\tau_2)\right],\\
\dot{y} &= z - \frac{\tau_3}{2}\left[(r_3 - s_3) + \sum_{j=-r_3}^{s_3} \tanh(z + j\tau_3)\right],\\
\dot{z} &= -ax - by - cz + a\frac{\tau_1}{2}\left[(r_1 - s_1) + \sum_{j=-r_1}^{s_1} \tanh(x + j\tau_1)\right] + b\frac{\tau_2}{2}\left[(r_2 - s_2) + \sum_{j=-r_2}^{s_2} \tanh(y + j\tau_2)\right]\\
&\quad + c\frac{\tau_3}{2}\left[(r_3 - s_3) + \sum_{j=-r_3}^{s_3} \tanh(z + j\tau_3)\right],
\end{aligned} \tag{11}$$

where a, b, c, τ_1, τ_2 and τ_3 are positive real values, whereas r_1, r_2, r_3, s_1, s_2, s_3 are non-negative integers. m, n and l are determined by

$$\begin{aligned}
m &= r_1 + s_1 + 2,\\
n &= r_2 + s_2 + 2,\\
l &= r_3 + s_3 + 2.
\end{aligned} \tag{12}$$

Similarly, define

$$\begin{aligned}
\Gamma_x &\approx \{s_1\tau_1, (s_1 - 1)\tau_1, \ldots, -r_1\tau_1\},\\
\Gamma_x^* &\approx \left\{(2s_1 + 1)\frac{\tau_1}{2}, (2s_1 - 1)\frac{\tau_1}{2}, \ldots, -(2r_1 + 1)\frac{\tau_1}{2}\right\},\\
\Gamma_y &\approx \{s_2\tau_2, (s_2 - 1)\tau_2, \ldots, -r_2\tau_2\},\\
\Gamma_y^* &\approx \left\{(2s_2 + 1)\frac{\tau_2}{2}, (2s_2 - 1)\frac{\tau_2}{2}, \ldots, -(2r_2 + 1)\frac{\tau_2}{2}\right\},\\
\Gamma_z &\approx \{s_3\tau_3, (s_3 - 1)\tau_3, \ldots, -r_3\tau_3\},\\
\Gamma_z^* &\approx \left\{(2s_3 + 1)\frac{\tau_3}{2}, (2s_3 - 1)\frac{\tau_3}{2}, \ldots, -(2r_3 + 1)\frac{\tau_3}{2}\right\}.
\end{aligned} \tag{13}$$

Then all equilibrium points of system (11) can be classified into the following eight different sets:

$$\begin{aligned}
\Gamma_1 &= \{(x, y, z) \mid x \in \Gamma_x^*,\ y \in \Gamma_y^*,\ z \in \Gamma_z^*\},\\
\Gamma_2 &= \{(x, y, z) \mid x \in \Gamma_x^*,\ y \in \Gamma_y,\ z \in \Gamma_z^*\},\\
\Gamma_3 &= \{(x, y, z) \mid x \in \Gamma_x,\ y \in \Gamma_y^*,\ z \in \Gamma_z^*\},\\
\Gamma_4 &= \{(x, y, z) \mid x \in \Gamma_x,\ y \in \Gamma_y,\ z \in \Gamma_z^*\},\\
\Gamma_5 &= \{(x, y, z) \mid x \in \Gamma_x^*,\ y \in \Gamma_y^*,\ z \in \Gamma_z\},\\
\Gamma_6 &= \{(x, y, z) \mid x \in \Gamma_x^*,\ y \in \Gamma_y,\ z \in \Gamma_z\},\\
\Gamma_7 &= \{(x, y, z) \mid x \in \Gamma_x,\ y \in \Gamma_y^*,\ z \in \Gamma_z\},\\
\Gamma_8 &= \{(x, y, z) \mid x \in \Gamma_x,\ y \in \Gamma_y,\ z \in \Gamma_z\}.
\end{aligned}$$

Calculations show that only the equilibrium points in sets Γ_1, Γ_4 and Γ_6 are saddle points of index two with eigenvalues satisfying $\lambda_1 < 0$ and $\lambda_{2,3} = \xi + \eta i$ ($\xi > 0$ and $\eta \neq 0$). These equilibrium points are responsible for the generation of $(r_1 + s_1 + 2) \times (r_2 + s_2 + 2) \times (r_3 + s_3 + 2)$ chaotic attractors. For example, choosing $a = b = c = 0.8$, $\tau_1 = 160$, $\tau_2 = 100$, $\tau_3 = 80$, and $r_1 = r_2 = r_3 = s_1 = s_2 = s_3 = 2$ in system (11), we obtain a $6 \times 6 \times 6$-grid-scroll chaotic attractor, as depicted in Fig. 5. The time history for the x component is shown in Fig. 6(a).

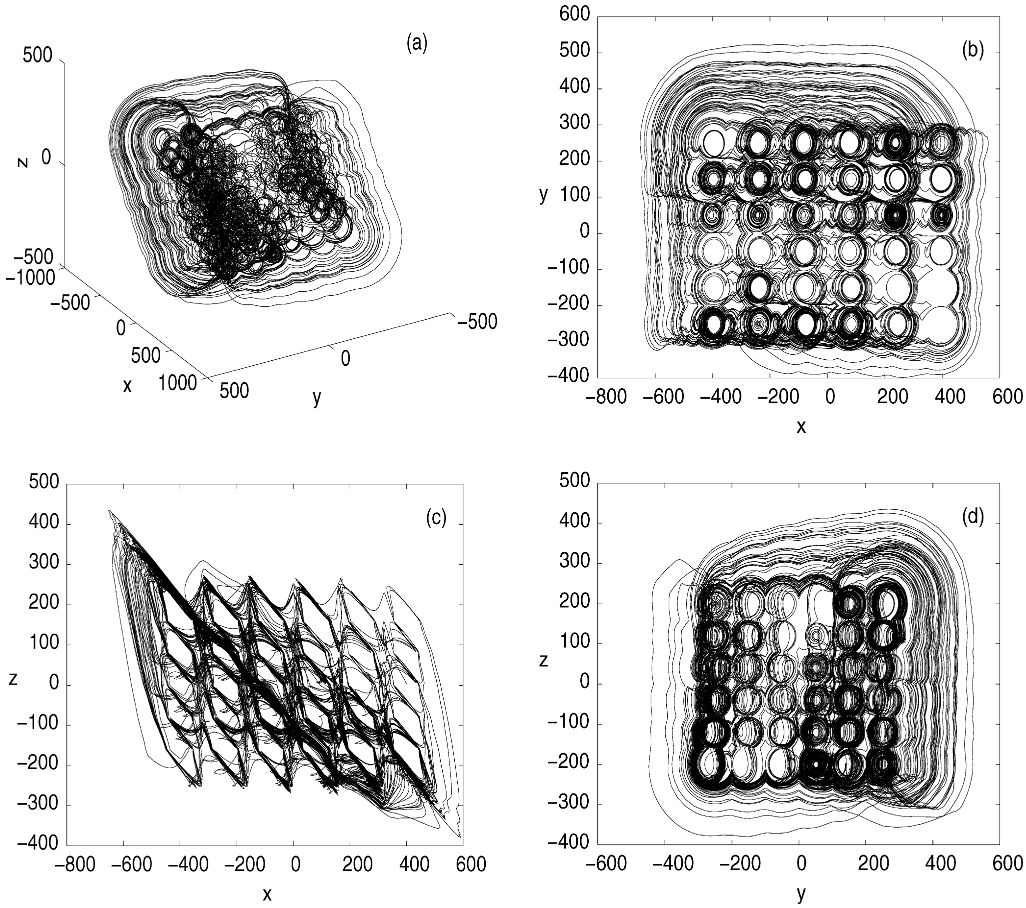

Fig. 5. Simulated results for 3-D $6 \times 6 \times 6$-scroll chaotic attractor of system (11) with $a = b = c = 0.8$, $\tau_1 = 160$, $\tau_2 = 100$, $\tau_3 = 80$, and $r_1 = t_2 = r_3 = s_1 = s_2 = s_3 = 2$: (a) the phase portrait in the x–y–z plane; (b) the phase portrait projected on the x–y plane; (c) the phase portrait projected on the x–z plane; (d) and the phase portrait projected on the y–z plane.

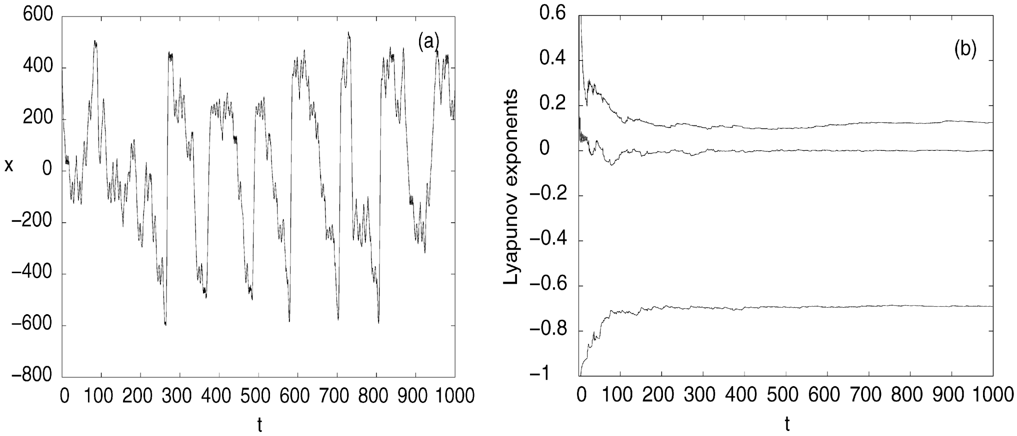

Fig. 6. Simulated results for 3-D $6 \times 6 \times 6$-scroll chaotic attractor of system (11) with $a = b = c = 0.8$, $\tau_1 = 160$, $\tau_2 = 100$, $\tau_3 = 80$, and $r_1 = r_2 = r_3 = s_1 = s_2 = s_3 = 2$: (a) the time history $x(t)$; and (b) the Lyapunov exponents.

Numerical computation gives the following three Lyapunov exponents for the system:

$$L_1 = 0.1256, \qquad L_2 = 0.0005, \qquad L_3 = -0.6916,$$

implying that the system generates a hyperchaos. The computation result of these Lyapunov exponents is shown in Fig. 6(b).

In system (11), letting $r_1 = s_1$, $r_2 = s_2$ and $r_3 = s_3$ yields

$$\begin{aligned}
\dot{x} &= y - \frac{\tau_2}{2} \sum_{j=-r_2}^{s_2} \tanh(y + j\tau_2), \\
\dot{y} &= z - \frac{\tau_3}{2} \sum_{j=-r_3}^{s_3} \tanh(z + j\tau_3), \\
\dot{z} &= -ax - by - cz + a\frac{\tau_1}{2} \sum_{j=-r_1}^{s_1} \tanh(x + j\tau_1) + b\frac{\tau_2}{2} \sum_{j=-r_2}^{s_2} \tanh(y + j\tau_2) + c\frac{\tau_3}{2} \sum_{j=-r_3}^{s_3} \tanh(z + j\tau_3).
\end{aligned} \tag{14}$$

Apparently, system (14) is symmetric about the origin, since the system is invariant under the transformation $(x, y, z) \to (-x, -y, -z)$. Therefore, system (14) with the given parameter values is a special case of system (11), as shown in Fig. 5.

6. Synchronization and stabilization of 1-D-*n*-scroll chaotic attractors

To further study the global and exponential synchronization of two 1-D-n-scroll chaotic attractors, consider system (4) as a drive system

$$\begin{aligned}
\dot{x}_d &= y_d, \\
\dot{y}_d &= z_d, \\
\dot{z}_d &= -ax_d - by_d - cz_d + a\frac{\tau}{2}\left[(r - s) + \sum_{j=-r}^{s} \tanh(x_d + j\tau)\right],
\end{aligned} \tag{15}$$

where the subscript d indicates the "drive." Then the corresponding driven (or receiving) system is

$$\begin{aligned}
\dot{x}_r &= y_r + u_1(x_d - x_r, y_d - y_r, z_d - z_r), \\
\dot{y}_r &= z_r + u_2(x_d - x_r, y_d - y_r, z_d - z_r), \\
\dot{z}_r &= -ax_r - by_r - cz_r + a\frac{\tau}{2}\left[(r - s) + \sum_{j=-r}^{s} \tanh(x_r + j\tau)\right] + u_3(x_d - x_r, y_d - y_r, z_d - z_r),
\end{aligned} \tag{16}$$

where the subscript r indicates the "receive." Here, u_i's are the continuous, linear functions of its variables, satisfying $u_i(0, 0, 0) = 0$, $i = 1, 2, 3$.

Let

$$e_x = x_d - x_r, \qquad e_y = y_d - y_r, \qquad e_z = z_d - z_r.$$

Then the error system is given by

$$\begin{aligned}
\dot{e}_x &= e_y - u_1(e_x, e_y, e_z), \\
\dot{e}_y &= e_z - u_2(e_x, e_y, e_z), \\
\dot{e}_z &= -ae_x - be_y - ce_z + a\frac{\tau}{2} \sum_{j=-r}^{s} f'(\xi)e_x - u_3(e_x, e_y, e_z),
\end{aligned} \tag{17}$$

where by the intermediate value theorem, $f'(\xi)e_x = \tanh(x_d + j\tau) - \tanh(x_r + j\tau)$ with $\min(x_r, x_d) < \xi < \max(x_r, x_d)$. We will use the property $(\tanh x)' = 1 - \tanh^2 x = \operatorname{sech}^2 x \leqslant 1 < +\infty$ to study the globally exponential synchronization and globally exponential stability.

Let $X^* = (x^*, y^*, z^*)$ denote any equilibrium point of system (4). Then, define $\bar{X} = X - X^* = (x - x^*, y - y^*, z - z^*)$. Thus system (17) can be rewritten as

$$\begin{aligned}
\dot{\bar{x}} &= \bar{y} - u_1(\bar{x}, \bar{y}, \bar{z}), \\
\dot{\bar{y}} &= \bar{z} - u_2(\bar{x}, \bar{y}, \bar{z}), \\
\dot{\bar{z}} &= -a\bar{x} - b\bar{y} - c\bar{z} + a\frac{\tau}{2} \sum_{j=-r}^{s} f'(\eta)\bar{x} - u_3(\bar{x}, \bar{y}, \bar{z}),
\end{aligned} \tag{18}$$

where η is a real value between x and x^*, and $f'(\eta)\bar{x} = \tanh(x + j\tau) - \tanh(x^* + j\tau)$.

Next, we will show that possibly the simplest feedback control laws u_1, u_2 and u_3 can be chosen such that the zero solution of the error system (17) or 18) is globally exponentially stabilized. Thus, systems (15) and (16) are globally exponentially synchronized, or the equilibrium point $X = X^*$ is globally exponentially stabilized.

Definition 1. With properly chosen feedback control laws u_i, $\forall(x_d(0), y_d(0), z_d(0)) \in R^3$ and corresponding $(x_r(0), y_r(0), z_r(0)) \in R^3$, if the zero solution of (17) is globally exponentially stabilized (globally asymptotically stabilized), then systems (15) and (16) are said to be globally exponentially synchronized (globally synchronized).

Definition 2. With properly chosen feedback control laws u_i, $\forall(x_d(0), y_d(0), z_d(0)) \in R^3$ and corresponding $(x_r(0), y_r(0), z_r(0)) \in R^3$, if the zero solution of (18) is globally exponentially stabilized (globally asymptotically stabilized), then the equilibrium point $X = X^*$ of system (4) is said to be globally exponentially stabilized (globally stabilized).

For convenience, we define two simple linear feedback control laws as follows:

$$u_1 = \delta_x e_x, \qquad u_2 = \delta_y e_y, \qquad u_3 = \delta_z e_z, \tag{19}$$

and

$$u_1 = \delta_x \bar{x}, \qquad u_2 = \delta_y \bar{y}, \qquad u_3 = \delta_z \bar{z}, \tag{20}$$

where δ_a, δ_y and δ_z are called control gain coefficients, to be specified in the following theorems and corollaries.

Theorem 1. *For system* (17), *under the control law* (19) *if one of the following conditions holds*:

(1) $\delta_x > 1$, $\delta_y > 1$, $\delta_z > a + b - c + a\frac{\tau}{2}(s + r + 1)$;
(2) $\delta_x > a + a\frac{\tau}{2}(s + r + 1)$, $\delta_y > b + 1$, $\delta_z > 1 - c$;

then the zero solution of (17) *is globally exponentially stabilized, and thus systems* (15) *and* (16) *are globally exponentially synchronized.*

Proof. Construct positive definite, radially unbounded vector Lyapunov function for system (17):

$$V = \left(|e_x|, |e_y|, |e_z|\right)^T.$$

Along the solution of system (17), evaluating the Dini derivative of V yields

$$\begin{pmatrix} D^+|e_x| \\ D^+|e_y| \\ D^+|e_z| \end{pmatrix}_{(17)} \leqslant \begin{bmatrix} -\delta_x & 1 & 0 \\ 0 & -\delta_y & 1 \\ a + a\frac{\tau}{2}(s + r + 1) & b & -c - \delta_z \end{bmatrix} \begin{pmatrix} |e_x| \\ |e_y| \\ |e_z| \end{pmatrix}. \tag{21}$$

Consider the comparison equation of system (21):

$$\begin{pmatrix} \dot{\eta}_x \\ \dot{\eta}_y \\ \dot{\eta}_z \end{pmatrix} = \begin{bmatrix} -\delta_x & 1 & 0 \\ 0 & -\delta_y & 1 \\ a + a\frac{\tau}{2}(s + r + 1) & b & -c - \delta_z \end{bmatrix} \begin{pmatrix} \eta_x \\ \eta_y \\ \eta_z \end{pmatrix} := A_1 \begin{pmatrix} \eta_x \\ \eta_y \\ \eta_z \end{pmatrix}, \tag{22}$$

which has the solution:

$$\begin{pmatrix} \eta_x(t) \\ \eta_y(t) \\ \eta_z(t) \end{pmatrix} = e^{A_1(t-t_0)} \begin{pmatrix} \eta_x(t_0) \\ \eta_y(t_0) \\ \eta_z(t_0) \end{pmatrix}.$$

If one of the conditions in Theorem 1 is satisfied, A_1 is a Hurwitz matrix [20]. Thus, there exist constants $M_1 \geqslant 1$, $\alpha_1 > 0$, satisfying

$$\left\| e^{A_1(t-t_0)} \right\| \leqslant M_1 e^{-\alpha_1(t-t_0)}.$$

By the comparison principal, we have

$$\left\| \begin{pmatrix} |e_x(t)| \\ |e_y(t)| \\ |e_z(t)| \end{pmatrix} \right\| \leqslant \left\| \begin{pmatrix} \eta_x(t) \\ \eta_y(t) \\ \eta_z(t) \end{pmatrix} \right\| \leqslant M_1 e^{-\alpha_1(t-t_0)} \left\| \begin{pmatrix} \eta_x(t_0) \\ \eta_y(t_0) \\ \eta_z(t_0) \end{pmatrix} \right\|. \tag{23}$$

Eq. (23) shows that the zero solution of system (17) is globally exponentially stabilized, and thus by Definition 1 we know that systems (15) and (16) are globally exponentially synchronized. □

Remark 1. One of the criteria in the control design is that the control should not alter the basic structure of the system. An extreme example of such control is the so-called "cancellation" control, which cancels terms on the right-hand side of the error system (17), or that of the controlled system (16).

For the control proposed in Theorem 1, substituting the feedback control (19) into Eq. (16) yields the following controlled system:

$$\begin{aligned}
\dot{x}_r &= y_r + \delta_x(x_d - x_r),\\
\dot{y}_r &= z_r + \delta_y(y_d - y_r),\\
\dot{z}_r &= -ax_r - by_r - cz_r + \delta_z(z_d - z_r) + a\frac{\tau}{2}\left[(r-s) + \sum_{j=-r}^{s}\tanh(x_r + j\tau)\right].
\end{aligned} \tag{24}$$

It is obvious that the original terms y_r and z_r in the first two equations of (24) are not canceled by the control. For the third equation, since the control gain δ_z is either great than $a+b-c+a\frac{\tau}{2}(s+r+1)$ or greater than $1-c$, the control term $-\delta_z z_r$ cannot cancel the original term z_r.

Next, we will present an example of "cancellation" control. Take the following linear control law:

$$u_1 = e_y + e_x, \qquad u_2 = e_z + e_y, \qquad u_3 = -(ae_x + be_y + ce_z) + e_z, \tag{25}$$

then the linear terms on the right-hand side of the error system (17) are all canceled and the resulting system becomes

$$\begin{aligned}
\dot{e}_x &= -e_x,\\
\dot{e}_y &= -e_y,\\
\dot{e}_x &= -e_z + \sum_{j=-r}^{s} a\frac{\tau}{2}f'(\xi)e_x,
\end{aligned} \tag{26}$$

which is globally asymptotically stable. However, substituting this control law into the corresponding system (17) cancel all the linear terms on the right-hand side of the system. Such control design (25) is not desirable from the view point of control theory.

Corollary 1. *For any given equilibrium point $X = X^*$ of system* (18), *choose the linear control law* (20). *Then if one of the following conditions is satisfied*:

(1) $\delta_x > 1$, $\delta_y > 1$, $\delta_z > a + b - c + a\frac{\tau}{2}(s+r+1)$;
(2) $\delta_x > a + a\frac{\tau}{2}(s+r+1)$, $\delta_y > b + 1$, $\delta_z > 1 - c$;

$X^* = (x^*, y^*, z^*)$ can be globally exponentially stabilized.

Remark 2. System (4) may have multiple equilibrium points. However, when the feedback control law (20) is applied, which is related to the equilibrium point $X^* = (x^*, y^*, z^*)$, all the other equilibrium points disappear. The only remaining one becomes the equilibrium point to be globally exponentially stabilized.

Theorem 2. *Choose the linear feedback control law* (19) *for system* (17). *Then under the conditions*:

$$\delta_x > \frac{1}{2} + \frac{a}{2b} + \frac{a\tau}{4b}(s+r+1), \qquad \delta_y > \frac{1}{2}, \qquad \delta_z > -c + \frac{a\tau}{4}(s+r+1) + \frac{a}{2},$$

the zero solution of the error system (17) *is globally exponentially stabilized, and thus systems* (15) *and* (16) *are globally exponentially synchronized.*

Proof. Construct positive definite, radially unbounded Lyapunov function for system (17):

$$V = \frac{1}{2}\left(e_x^2 + e_y^2 + \frac{e_z^2}{b}\right) = \begin{pmatrix} e_x \\ e_y \\ e_z \end{pmatrix}^T P \begin{pmatrix} e_x \\ e_y \\ e_z \end{pmatrix}.$$

Let $\lambda_m(P)$ and $\lambda_M(P)$ denote the minimum and maximum eigenvalues of

$$P = \begin{bmatrix} \frac{1}{2} & 0 & 0 \\ 0 & \frac{1}{2} & 0 \\ 0 & 0 & \frac{1}{2b} \end{bmatrix},$$

respectively. Then we have

$$\begin{aligned}
\left.\frac{dV}{dt}\right|_{(17)} &= e_x\dot{e}_x + e_y\dot{e}_y + \frac{1}{b}e_z\dot{e}_z \\
&\leqslant \begin{pmatrix} |e_x| \\ |e_y| \\ |e_z| \end{pmatrix}^T \begin{bmatrix} -\delta_x & \frac{1}{2} & \frac{a}{2b} + \frac{a\tau}{4b}(r+s+1) \\ \frac{1}{2} & -\delta_y & 0 \\ \frac{a}{2b} + \frac{a\tau}{4b}(r+s+1) & 0 & -\frac{c+\delta_z}{b} \end{bmatrix} \begin{pmatrix} |e_x| \\ |e_y| \\ |e_z| \end{pmatrix} \\
&:= \begin{pmatrix} |e_x| \\ |e_y| \\ |e_z| \end{pmatrix}^T A_2 \begin{pmatrix} |e_x| \\ |e_y| \\ |e_z| \end{pmatrix} \\
&\leqslant \lambda_M(A_2)\big(e_x^2 + e_y^2 + e_z^2\big),
\end{aligned}$$

where $\lambda_M(A_2)$ is the maximum eigenvalue of A_2. It follows from the conditions in Theorem 2 that $\lambda_M(A_2) < 0$. Hence,

$$\frac{dV}{dt} \leqslant \lambda_M(A_2)\frac{\lambda_M(P)}{\lambda_M(P)}\big(e_x^2 + e_y^2 + e_z^2\big) \leqslant \frac{\lambda_M(A_2)}{\lambda_M(P)}V,$$

which implies that

$$V\big(X(t)\big) \leqslant V\big(X(t_0)\big)e^{\frac{\lambda_M(A_2)}{\lambda_M(P)}(t-t_0)}.$$

Hence,

$$e_x^2(t) + e_y^2(t) + e_z^2(t) \leqslant \frac{V(X(t))}{\lambda_m(P)} \leqslant \frac{V(X(t_0))}{\lambda_m(P)}e^{\frac{\lambda_M(A_2)}{\lambda_M(P)}(t-t_0)}. \tag{27}$$

Eq. (27) shows that the zero solution of (17) is globally exponentially stabilized, and thus systems (15) and (16) are globally exponentially synchronized. □

Corollary 2. *For any given equilibrium point $X = X^*$ of system* (4)*, choose the feedback control law* (20)*. If*

$$\delta_x > \frac{1}{2} + \frac{a}{2b} + \frac{a\tau}{4b}(s+r+1), \qquad \delta_y > \frac{1}{2}, \qquad \delta_z > -c + \frac{a\tau}{4}(s+r+1) + \frac{a}{2},$$

then the equilibrium point of system (4)*, $X = X^*$, is globally exponentially stabilized.*

The proof of Corollary 2 is similar to that of Theorem 2.

Theorem 3. *Choose the linear feedback control law* (19) *for system* (17)*. When*

$$\delta_x > a + a\frac{\tau}{2}(r+s+1), \qquad \delta_y = 1 + b, \qquad \delta_z = 1 - c,$$

the zero solution of (17) *is globally exponentially stabilized, i.e., the two systems* (15) *and* (16) *are globally exponentially synchronized.*

Proof. Construct positive definite, radially unbounded Lyapunov function for Eq. (17):

$$V = |e_x| + |e_y| + |e_z|.$$

Then we have

$$\begin{aligned}
D^+V|_{(17)} &= \dot{e}_x \operatorname{sign} e_x + \dot{e}_y \operatorname{sign} e_y + \dot{e}_z \operatorname{sign} e_z \\
&\leqslant |e_y| + |e_z| - \delta_x|e_x| - \delta_y|e_y| - \delta_z|e_z| - c|e_z| + a\frac{\tau}{2}(r+s+1)|e_x| + a|e_x| + b|e_y| \\
&\leqslant \left(-\delta_x + a + a\frac{\tau}{2}(r+s+1)\right)|e_x| + (-\delta_y + b + 1)|e_y| + (-\delta_z - c + 1)|e_z| \\
&= \left(-\delta_x + a + a\frac{\tau}{2}(r+s+1)\right)|e_x|,
\end{aligned} \tag{28}$$

which implies that the zero solution of (17) is globally exponentially stabilized with respect to the partial variable e_x.

Next, we consider the coefficient matrix of the linear part of system (17) with the feedback control law given in Theorem 3:

$$A_3 = \begin{bmatrix} -\delta_x & 1 & 0 \\ 0 & -\delta_y & 1 \\ -a & -b & -1 \end{bmatrix}$$

from which we obtain the characteristic polynomial:

$$\begin{aligned}
\det(\lambda I_3 - A_3) &= \det\begin{bmatrix} \lambda+\delta_x & -1 & 0 \\ 0 & \lambda+1+b & -1 \\ a & b & \lambda+1 \end{bmatrix} \\
&= \lambda^3 + (b+2+\delta_x)\lambda^2 + \big[\delta_x(b+2)+2b+1\big]\lambda + \delta_x(2b+1)+a \\
&:= \lambda^3 + p\lambda^2 + q\lambda + r.
\end{aligned}$$

It is well known that the sufficient and necessary condition for A_3 to be a Hurwitz matrix is

$$p>0, \qquad pq>r>0.$$

Using $a=b$, we have

$$\begin{aligned}
pq &= (b+2+\delta_x)\big[\delta_x(b+2)+2b+1\big] \\
&= (b+2)(b+1) + \delta_x(b+2)^2 + b(b+2) + \delta_x(b+1) + \delta_x^2(b+2) + b\delta_x \\
&> \delta_x(2b+1)+b \\
&= r > 0,
\end{aligned} \tag{29}$$

which implies that A_3 is a Hurwitz matrix.

On the other hand, the solution of (17) can be written as

$$\begin{pmatrix} e_x(t) \\ e_y(t) \\ e_z(t) \end{pmatrix} = e^{A_3(t-t_0)} \begin{pmatrix} e_x(t_0) \\ e_y(t_0) \\ e_z(t_0) \end{pmatrix} + \int_{t_0}^{t} e^{A_3(t-\tau)} \begin{pmatrix} 0 \\ 0 \\ a\frac{\tau}{2}\sum_{j=-r}^{s} f'(\xi)e_x(\tau) \end{pmatrix} d\tau.$$

Since A_3 is a Hurwitz matrix, there exist constants $M_1 \geqslant 1$ and $\alpha_1 > 0$ satisfying

$$\big\| e^{A_3(t-t_0)} \big\| \leqslant M_1 e^{-\alpha_1(t-t_0)}.$$

Thus,

$$\left\| \begin{pmatrix} e_x(t) \\ e_y(t) \\ e_z(t) \end{pmatrix} \right\| \leqslant M_1 \left\| \begin{pmatrix} e_x(t_0) \\ e_y(t_0) \\ e_z(t_0) \end{pmatrix} \right\| e^{-\alpha_1(t-t_0)} + \int_{t_0}^{t} M_1 e^{-\alpha_1(t-\tau)} a\frac{\tau}{2}(s+r+1)\big\|e_x(\tau)\big\|\, d\tau.$$

With the property $\lim_{t\to\infty} e_x(t) = 0$, we can prove that $\forall\varepsilon>0$, $\exists\sigma_1>0$, when $\|e_x(t_0), e_y(t_0), e_z(t_0)\| \leqslant \sigma_1$,

$$M_1 \left\| \begin{pmatrix} e_x(t_0) \\ e_y(t_0) \\ e_z(t_0) \end{pmatrix} \right\| e^{-\alpha_1(t-t_0)} < \frac{\varepsilon}{3}.$$

Moreover, for any $t_1 > t_0$, when $\|e_x(t_0), e_y(t_0), e_z(t_0)\| \leqslant \sigma_1$, we have

$$\int_{t_0}^{t_1} M_1 e^{-\alpha_1(t-\tau)} a\frac{\tau}{2}(s+r+1)\big\|e_x(\tau)\big\| d\tau < \frac{\varepsilon}{3},$$

and

$$\int_{t_1}^{t} M_1 e^{-\alpha_1(t-\tau)} a\frac{\tau}{2}(s+r+1)\big\|e_x(\tau)\big\|\, d\tau < \frac{\varepsilon}{3}.$$

Therefore,

$$\begin{aligned}
\left\| \begin{pmatrix} e_x(t) \\ e_y(t) \\ e_z(t) \end{pmatrix} \right\| &\leqslant M_1 \left\| \begin{pmatrix} e_x(t_0) \\ e_y(t_0) \\ e_z(t_0) \end{pmatrix} \right\| e^{-\alpha_1(t-t_0)} + \int_{t_0}^{t_1} M_1 e^{-\alpha_1(t-\tau)} a\frac{\tau}{2}(s+r+1)\big\|e_x(\tau)\big\|\, d\tau \\
&\quad + \int_{t_1}^{t} M_1 e^{-\alpha_1(t-\tau)} a\frac{\tau}{2}(s+r+1)\big\|e_x(\tau)\big\|\, d\tau \\
&< \frac{\varepsilon}{3} + \frac{\varepsilon}{3} + \frac{\varepsilon}{3} = \varepsilon.
\end{aligned}$$

For any $(e_x(t_0), e_y(t_0), e_z(t_0)) \in R^3$, it is easy to show that

$$\lim_{t\to\infty} M_1 \left\| \begin{pmatrix} e_x(t_0) \\ e_y(t_0) \\ e_z(t_0) \end{pmatrix} \right\| e^{-\alpha_1(t-t_0)} + \lim_{t\to\infty} \int_{t_0}^{t} M_1 e^{-\alpha_1(t-\tau)} a\frac{\tau}{2}(s+r+1)\left\|e_x(\tau)\right\| d\tau = 0. \tag{30}$$

Thus, the zero solution of (17) is globally asymptotically stabilized, and so systems (15) and (16) are globally exponentially synchronized. □

Corollary 3. *For any equilibrium point $X = X^*$ of system* (4)*, choose the linear feedback control law* (20)*. When*

$$\delta_x > a + a\frac{\tau}{2}(r+s+1), \qquad \delta_y = 1+b, \qquad \delta_z = 1-c,$$

X^* can be globally exponentially stabilized.

7. Synchronization and stabilization of 2-D-$m \times n$-grid-scroll chaotic attractors

In this section, we consider synchronization and stabilization of the 2-D-$m \times n$-grid-scroll chaotic attractors. Assume that the drive system is

$$\begin{aligned}
\dot{x}_d &= y_d - \frac{\tau_2}{2}\left[(r_2-s_2) + \sum_{j=-r_2}^{s_2} \tanh(y_d + j\tau_2)\right], \\
\dot{y}_d &= z_d, \\
\dot{z}_d &= -ax_d - by_d - cz_d + \frac{a\tau_1}{2}\left[(r_1-s_1) + \sum_{j=-r_1}^{s_1} \tanh(x_d + j\tau_1)\right] + \frac{b\tau_2}{2}\left[(r_2-s_2) + \sum_{j=-r_2}^{s_2} \tanh(y_d + j\tau_2)\right],
\end{aligned} \tag{31}$$

while, the corresponding driven system is given by

$$\begin{aligned}
\dot{x}_r &= y_r - \frac{\tau_2}{2}\left[(r_2-s_2) + \sum_{j=-r_2}^{s_2} \tanh(y_r + j\tau_2)\right] + u_1(e_x, e_y, e_z), \\
\dot{y}_r &= z_r + u_2(e_x, e_y, e_z), \\
\dot{z}_r &= -ax_r - by_r - cz_r + \frac{a\tau_1}{2}\left[(r_1-s_1) + \sum_{j=-r_1}^{s_1} \tanh(x_r + j\tau_1)\right] + \frac{b\tau_2}{2}\left[(r_2-s_2) + \sum_{j=-r_2}^{s_2} \tanh(y_r + j\tau_2)\right] \\
&\quad + u_3(e_x, e_y, e_z).
\end{aligned} \tag{32}$$

The error system is then obtained as

$$\begin{aligned}
\dot{e}_x &= e_y - \frac{\tau_2}{2}\sum_{j=-r_2}^{s_2} f'(\xi)e_y - u_1(e_x, e_y, e_z), \\
\dot{e}_y &= e_z - u_2(e_x, e_y, e_z), \\
\dot{e}_z &= -ae_x - be_y - ce_z + \frac{a\tau_1}{2}\sum_{j=-r_1}^{s_1} f'(\xi)e_x + \frac{b\tau_2}{2}\sum_{j=-r_2}^{s_2} f'(\xi)e_y - u_3(e_x, e_y, e_z).
\end{aligned} \tag{33}$$

Theorem 4. *In system* (33)*, choose the linear control law* (19)*. If one of the following conditions is satisfied*:

(1) $\delta_x > 1 + \frac{\tau_2}{2}(s_2+r_2+1)$, $\delta_y > 1$, $\delta_z > a + \frac{a\tau_1}{2}(s_1+r_1+1) + b + \frac{b\tau_2}{2}(s_2+r_2+1) - c$;
(2) $\delta_x > a + \frac{a\tau_1}{2}(s_1+r_1+1)$, $\delta_y > 1 + \frac{\tau_2}{2}(s_2+r_2+1) + b + \frac{b\tau_2}{2}(s_2+r_2+1)$, $\delta_z > 1-c$;

then the zero solution of (33) *is globally exponentially stabilized, and thus systems* (31) *and* (32) *are globally exponentially synchronized.*

Proof. We construct positive definite, radially unbounded vector Lyapunov function:

$$V = \left(|e_x|, |e_y|, |e_z|\right)^T,$$

and then we have

$$D^+V\mid_{(33)}=\begin{pmatrix} D^+|e_x| \\ D^+|e_y| \\ D^+|e_z| \end{pmatrix}_{(33)} \leqslant \begin{bmatrix} -\delta_x & 1+\frac{\tau_2}{2}(s_2+r_2+1) & 0 \\ 0 & -\delta_y & 1 \\ a+\frac{a\tau_1}{2}(s_1+r_1+1) & b+\frac{b\tau_2}{2}(s_2+r_2+1) & -\delta_z-c \end{bmatrix} \begin{pmatrix} |e_x| \\ |e_y| \\ |e_z| \end{pmatrix} := A_4 \begin{pmatrix} |e_x| \\ |e_y| \\ |e_z| \end{pmatrix}. \tag{34}$$

Consider the comparison equation of (34), given by

$$\begin{pmatrix} \dot\eta_x \\ \dot\eta_y \\ \dot\eta_z \end{pmatrix} = \begin{bmatrix} -\delta_x & 1+\frac{\tau_2}{2}(s_2+r_2+1) & 0 \\ 0 & -\delta_y & 1 \\ a+\frac{a\tau_1}{2}(s_1+r_1+1) & b+\frac{b\tau_2}{2}(s_2+r_2+1) & -\delta_z-c \end{bmatrix} \begin{pmatrix} \eta_x \\ \eta_y \\ \eta_z \end{pmatrix} := A_4 \begin{pmatrix} \eta_x \\ \eta_y \\ \eta_z \end{pmatrix}. \tag{35}$$

The solution of Eq. (35) can be written as

$$\begin{pmatrix} \eta_x(t) \\ \eta_y(t) \\ \eta_z(t) \end{pmatrix} = e^{A_4(t-t_0)} \begin{pmatrix} \eta_x(t_0) \\ \eta_y(t_0) \\ \eta_z(t_0) \end{pmatrix}.$$

From the conditions of the Theorem 4, we know that A_4 is a Hurwitz matrix. Hence, there exist $M_4 \geqslant 1$ and $\alpha_4 > 0$ such that

$$\left\| e^{A_4(t-t_0)} \right\| \leqslant M_4 e^{-\alpha_4(t-t_0)}.$$

Further, from the comparison principle we know that

$$\begin{aligned} \left\| \left(|e_x(t)|, |e_y(t)|, |e_z(t)| \right)^T \right\| &\leqslant \left\| \left(\eta_x(t), \eta_y(t), \eta_z(t) \right)^T \right\| \\ &\leqslant \left\| e^{A_4(t-t_0)} \right\| \left\| \left(\eta_x(t_0), \eta_y(t_0), \eta_z(t_0) \right)^T \right\| \\ &\leqslant M_4 e^{-\alpha_4(t-t_0)} \left\| \left(\eta_x(t_0), \eta_y(t_0), \eta_z(t_0) \right)^T \right\|, \end{aligned} \tag{36}$$

which indicates that the conclusion of Theorem 4 is true. □

Corollary 4. *For any given equilibrium point $X = X^*$ of system* (6), *if choose the linear feedback control law* (20), *where the control gain coefficients δ_x, δ_y and δ_z satisfy the conditions in Theorem* 4, *the zero solution of the following error system*

$$\begin{aligned} \dot{\bar x} &= \bar y - \frac{\tau_2}{2}\sum_{j=-r_2}^{s_2} f'(\xi)\bar y - u_1(\bar x, \bar y, \bar z), \\ \dot{\bar y} &= \bar z - u_2(\bar x, \bar y, \bar z), \\ \dot{\bar z} &= -a\bar x - b\bar y - c\bar z + \frac{a\tau_1}{2}\sum_{j=-r_1}^{s_1} f'(\xi)\bar x + \frac{b\tau_2}{2}\sum_{j=-r_2}^{s_2} f'(\xi)\bar y - u_3(\bar x, \bar y, \bar z) \end{aligned} \tag{37}$$

is globally exponentially stabilized, i.e., the equilibrium point $X^* = (x^*, y^*, z^*)$ is globally exponentially stabilized.

Theorem 5. *In system* (33), *again choose the linear control law* (19)*. If*

$$\begin{aligned} \delta_x &> 1 + \frac{\tau_2}{4}(s_2+r_2+1) + \frac{\tau_1}{4}(s_1+r_1+1), \\ \delta_y &> 1 + \frac{\tau_2}{4}(s_2+r_2+1) + \frac{b\tau_2}{4a}(s_2+r_2+1) + \frac{b}{2a}, \end{aligned}$$

and

$$\delta_z > a + \frac{b}{2} + \frac{a\tau_1}{4}(r_1+s_1+1) + \frac{b\tau_2}{4}(r_2+s_2+1) - c,$$

then the zero solution of (33) *is globally exponentially stabilized. Thus, systems* (31) *and* (32) *are globally exponentially synchronized.*

Proof. Construct the positive definite, radially unbounded Lyapunov function:

$$V = \frac{1}{2}\left(e_x^2 + e_y^2 + \frac{e_z^2}{a} \right).$$

Then we have

$$
\begin{aligned}
\left.\frac{dV}{dt}\right|_{(33)} &\leqslant -\delta_x e_x^2 + e_x e_y + \frac{\tau_2}{2}(s_2+r_2+1)|e_x||e_y| + e_y e_z - \delta_y e_y^2 - e_x e_z - \frac{b}{a}e_y e_z - \frac{c}{a}e_z^2 - \frac{\delta_z e_z^2}{a} \\
&\quad + \frac{\tau_1}{2}(s_1+r_1+1)|e_x||e_z| + \frac{b\tau_2}{2a}(s_2+r_2+1)|e_y||e_z| \\
&\leqslant \begin{pmatrix} |e_x| \\ |e_y| \\ |e_z| \end{pmatrix}^T
\begin{bmatrix}
-\delta_x & \frac{1}{2}+\frac{\tau_2}{4}(s_2+r_2+1) & \frac{1}{2}+\frac{\tau_1}{4}(s_1+r_1+1) \\
\frac{1}{2}+\frac{\tau_2}{4}(s_2+r_2+1) & -\delta_y & \frac{1}{2}+\frac{b}{2a} + \frac{b\tau_2}{4a}(s_2+r_2+1) \\
\frac{1}{2}+\frac{\tau_1}{4}(s_1+r_1+1) & \frac{1}{2}+\frac{b}{2a} + \frac{b\tau_2}{4a}(r_2+s_2+1) & -\frac{c}{a}-\frac{\delta_z}{a}
\end{bmatrix}
\begin{pmatrix} |e_x| \\ |e_y| \\ |e_z| \end{pmatrix} \\
&:= \begin{pmatrix} |e_x| \\ |e_y| \\ |e_z| \end{pmatrix}^T A_5 \begin{pmatrix} |e_x| \\ |e_y| \\ |e_z| \end{pmatrix}.
\end{aligned}
$$

From the proposed conditions we know that A_5 is negative definite. Similar to the proof of Theorem 2, it is easy to show that

$$
e_x^2(t) + e_y^2(t) + e_z^2(t) \leqslant \frac{V(X(t))}{\lambda_m(P)} \leqslant \frac{V(X(t_0))}{\lambda_m(P)} e^{\frac{\lambda_M(A_5)}{\lambda_M(P)}(t-t_0)}, \tag{38}
$$

indicating that the conclusion of Theorem 5 is true. □

Corollary 5. *For any given equilibrium point $X = X^*$ of system* (31)*, under the linear control law* (20)*, when the conditions in Theorem* 5 *hold, the zero solution of system* (37) *is globally exponentially stable. Thus the equilibrium point $X = X^*$ of* (31) *is globally exponentially stabilized.*

8. Synchronization and stabilization of 3-D-$m \times n \times l$-grid-scroll chaotic attractors

In this section, we study synchronization and stabilization of the 3-D-$m \times n \times l$-grid-scroll chaotic attractors. For this case, the drive system is

$$
\begin{aligned}
\dot{x}_d &= y_d - \frac{\tau_2}{2}\left[(r_2-s_2) + \sum_{j=-r_2}^{s_2}\tanh(y_d+j\tau_2)\right], \\
\dot{y}_d &= z_d - \frac{\tau_3}{2}\left[(r_3-s_3) + \sum_{j=-r_3}^{s_3}\tanh(z_d+j\tau_3)\right], \\
\dot{z}_d &= -ax_d - by_d - cz_d + \frac{a\tau_1}{2}\left[(r_1-s_1) + \sum_{j=-r_1}^{s_1}\tanh(x_d+j\tau_1)\right] + \frac{b\tau_2}{2}\left[(r_2-s_2) + \sum_{j=-r_2}^{s_2}\tanh(y_d+j\tau_2)\right] \\
&\quad + \frac{c\tau_3}{2}\left[(r_3-s_3) + \sum_{j=-r_2}^{s_2}\tanh(z_d+j\tau_3)\right],
\end{aligned} \tag{39}
$$

while the corresponding driven system with controls is described by

$$
\begin{aligned}
\dot{x}_r &= y_r - \frac{\tau_2}{2}\left[(r_2-s_2) + \sum_{j=-r_2}^{s_2}\tanh(y_r+j\tau_2)\right] + u_1(e_x,e_y,e_z), \\
\dot{y}_r &= z_r - \frac{\tau_3}{2}\left[(r_3-s_3) + \sum_{j=-r_3}^{s_3}\tanh(z_r+j\tau_3)\right] + u_2(e_x,e_y,e_z), \\
\dot{z}_r &= -ax_r - by_r - cz_r + \frac{a\tau_1}{2}\left[(r_1-s_1) + \sum_{j=-r_1}^{s_1}\tanh(x_r+j\tau_1)\right] + \frac{b\tau_2}{2}\left[(r_2-s_2) + \sum_{j=-r_2}^{s_2}\tanh(y_r+j\tau_2)\right] \\
&\quad + \frac{c\tau_3}{2}\left[(r_3-s_3) + \sum_{j=-r_3}^{s_3}\tanh(z_r+j\tau_3)\right] + u_3(e_x,e_y,e_z).
\end{aligned} \tag{40}
$$

The error system can then be obtained as

$$\dot{e}_x = e_y - \frac{\tau_2}{2}\sum_{j=-r_2}^{s_2} f'(\xi)e_y - u_1(e_x, e_y, e_z),$$
$$\dot{e}_y = e_z - \frac{\tau_3}{2}\sum_{j=-r_3}^{s_3} f'(\xi)e_z - u_2(e_x, e_y, e_z),$$
$$\dot{e}_z = -ae_x - be_y - ce_z + \frac{a\tau_1}{2}\sum_{j=-r_1}^{s_1} f'(\xi)e_x + \frac{b\tau_2}{2}\sum_{j=-r_2}^{s_2} f'(\xi)e_y + \frac{c\tau_3}{2}\sum_{j=-r_3}^{s_3} f'(\xi)e_z - u_3(e_x, e_y, e_z). \tag{41}$$

Theorem 6. *In system* (41), *choose the linear feedback control law* (19). *If $\delta_x \geqslant 0$, $\delta_y \geqslant 0$ and $\delta_z \geqslant 0$ are properly chosen such that*

$$A_6 = \begin{bmatrix} -\delta_x & 1 + \frac{\tau_2}{2}(s_2 + r_2 + 1) & 0 \\ 0 & -\delta_y & 1 + \frac{\tau_3}{2}(s_3 + r_3 + 1) \\ \frac{a\tau_1}{2}(s_1 + r_1 + 1) + a & \frac{b\tau_2}{2}(s_2 + r_2 + 1) + b & -\delta_z - c + \frac{c\tau_3}{2}(s_3 + r_3 + 1) \end{bmatrix}$$

is a Hurwitz matrix, then the zero solution of (41) *is globally exponentially stable. Thus, systems* (39) *and* (40) *are globally exponentially synchronized.*

Proof. Construct positive definite, radially unbounded vector Lyapunov function:

$$V = \big(|e_x|, |e_y|, |e_z|\big)^T.$$

Then we have

$$\begin{aligned} D^+V|_{(41)} &= \begin{pmatrix} D^+|e_x| \\ D^+|e_y| \\ D^+|e_z| \end{pmatrix} \\ &\leqslant \begin{bmatrix} -\delta_x & 1 + \frac{\tau_2}{2}(s_2 + r_2 + 1) & 0 \\ 0 & -\delta_y & 1 + \frac{\tau_3}{2}(s_3 + r_3 + 1) \\ \frac{a\tau_1}{2}(s_1 + r_1 + 1) + a & \frac{b\tau_2}{2}(s_2 + r_2 + 1) + b & -\delta_z - c + \frac{c\tau_3}{2}(s_3 + r_3 + 1) \end{bmatrix} \begin{pmatrix} |e_x| \\ |e_y| \\ |e_z| \end{pmatrix} \\ &:= A_6 \begin{pmatrix} |e_x| \\ |e_y| \\ |e_z| \end{pmatrix}. \end{aligned} \tag{42}$$

Consider the comparison equation of (42):

$$\begin{pmatrix} \dot{\eta}_x \\ \dot{\eta}_y \\ \dot{\eta}_z \end{pmatrix} = \begin{bmatrix} -\delta_x & 1 + \frac{\tau_2}{2}(s_2 + r_2 + 1) & 0 \\ 0 & -\delta_y & 1 + \frac{\tau_3}{2}(s_3 + r_3 + 1) \\ \frac{a\tau_1}{2}(s_1 + r_1 + 1) + a & \frac{b\tau_2}{2}(s_2 + r_2 + 1) + b & -\delta_z - c + \frac{c\tau_3}{2}(s_3 + r_3 + 1) \end{bmatrix} \begin{pmatrix} \eta_x \\ \eta_y \\ \eta_z \end{pmatrix} := A_6 \begin{pmatrix} \eta_x \\ \eta_y \\ \eta_z \end{pmatrix}. \tag{43}$$

Since A_6 is a Hurwitz matrix, there exist $M_6 \geqslant 1$ and $\alpha_6 > 0$ such that

$$\big\| \big(|e_x|, |e_y|, |e_z|\big)^T \big\| \leqslant \big\| (\eta_x, \eta_y, \eta_z)^T \big\| \leqslant M_6 e^{-\alpha_6(t-t_0)} \big\| \big(\eta_x(t_0), \eta_y(t_0), \eta_z(t_0)\big)^T \big\|,$$

indicating that the conclusion of Theorem 6 is true. □

Theorem 7. *In system* (41), *choose the same linear control law as that for the proof of Theorem* 6. *If*

$$A_7 = \begin{bmatrix} -\delta_x & \frac{1}{2} + \frac{\tau_2}{4}(s_2 + r_2 + 1) & \frac{1}{2} + \frac{\tau_1}{4}(s_1 + r_1 + 1) \\ \frac{1}{2} + \frac{\tau_2}{4}(s_2 + r_2 + 1) & -\delta_y & \frac{a+b}{2a} + \frac{\tau_3}{4}(s_3 + r_3 + 1) \\ & & \frac{b\tau_2}{4a}(s_2 + r_2 + 1) \\ \frac{1}{2} + \frac{\tau_1}{4}(s_1 + r_1 + 1) & \frac{a+b}{2a} + \frac{\tau_3}{4}(s_3 + r_3 + 1) & -\frac{c}{a} + \frac{c\tau_3}{2a}(s_3 + r_3 + 1) - \frac{\delta_z}{a} \\ & \frac{b\tau_2}{4a}(s_2 + r_2 + 1) & \end{bmatrix}$$

is a Hurwitz matrix, then the zero solution of system (41) *is globally exponentially stable. Thus, systems* (39) *and* (40) *are globally exponentially synchronized.*

Proof. We use the same Lyapunov function as that in the proof of Theorem 5:

$$V = \frac{1}{2}\left(e_x^2 + e_y^2 + \frac{e_z^2}{a}\right)$$

and then we obtain

$$\begin{aligned}\frac{dV}{dt}\bigg|_{(41)} &\leqslant |e_xe_y| + \frac{\tau_2}{2}(s_2+r_2+1)|e_xe_y| - \delta_x e_x^2 + |e_ye_z| + \frac{\tau_3}{2}(s_3+r_3+1)|e_ye_z| - \delta_y e_y^2 + |e_xe_z| + \frac{b}{a}|e_ye_z| - \frac{c}{a}e_z^2 \\ &\quad + \frac{\tau_1}{2}(s_1+r_1+1)|e_xe_z| + \frac{b\tau_2}{2a}(s_2+r_2+1)|e_ye_z| + \frac{c\tau_3}{2a}(s_3+r_3+1)e_z^2 - \frac{1}{a}\delta_z e_z^2 \\ &= \begin{pmatrix}|e_x|\\|e_y|\\|e_z|\end{pmatrix}^T A_7 \begin{pmatrix}|e_x|\\|e_y|\\|e_z|\end{pmatrix},\end{aligned} \tag{44}$$

implying

$$\left(e_x^2(t)+e_y^2(t)+e_z^2(t)\right) \leqslant \frac{V(X(t))}{\lambda_m(P)} \leqslant \frac{V(X(t_0))}{\lambda_m(P)} e^{\frac{\lambda_M(A_7)}{\lambda_M(P)}(t-t_0)},$$

where the definitions of $\lambda_M(P)$, $\lambda_m(P)$ and $\lambda_M(A_7)$ are similar to those used in Theorem 2. Thus, the conclusion is true. □

Corollary 6. *If the conditions in Theorems* 6 *and* 7 *hold, the zero solution of the following system*

$$\begin{aligned}\dot{\bar{x}} &= -\delta_x\bar{x} + \bar{y} - \frac{\tau_2}{2}\sum_{j=-r_2}^{s_2} f'(\eta)\bar{y}, \\ \dot{\bar{y}} &= -\delta_y\bar{y} - \frac{\tau_3}{2}\sum_{j=-r_3}^{s_3} f'(\eta)\bar{z}, \\ \dot{\bar{z}} &= -(\delta_z+c)\bar{z} - a\bar{x} - b\bar{y} + \frac{a\tau_1}{2}\sum_{j=-r_1}^{s_1} f'(\eta)\bar{x} + \frac{b\tau_2}{2}\sum_{j=-r_2}^{s_2} f'(\eta)\bar{y} + \frac{c\tau_3}{2}\sum_{j=-r_3}^{s_3} f'(\eta)\bar{z}\end{aligned} \tag{45}$$

is globally exponentially stable. Thus the equilibrium point $X = X^*$ is globally exponentially stabilized.

9. Numerical simulation examples

In this section, we present some numerical examples to demonstrate the applicability of control laws proposed in the previous sections. The analytical predictions for the control laws are verified by numerical simulations.

For the synchronization problem, we show three examples for 1-D, 2-D and 3-D multi-scroll chaotic systems using the control laws given in Theorems 3, 4 and 6, respectively, since the remaining cases are similar. The initial conditions chosen respectively for 1-D, 2-D and 3-D systems are:

$$x_d(0) = 4, \qquad y_d(0) = 2, \qquad z_d(0) = 2, \tag{46}$$

and

$$x_r(0) = 1, \qquad y_r(0) = 5, \qquad z_r(0) = 3 \tag{47}$$

for the 1-D system;

$$x_d(0) = 10, \qquad y_d(0) = 5, \qquad z_d(0) = 5, \tag{48}$$

and

$$x_r(0) = 15, \qquad y_r(0) = 8, \qquad z_r(0) = 2 \tag{49}$$

for the 2-D system; and

$$x_d(0) = 10, \qquad y_d(0) = 12, \qquad z_d(0) = 1, \tag{50}$$

and

$$x_r(0) = 8, \qquad y_r(0) = 15, \qquad z_r(0) = 4 \tag{51}$$

for the 3-D system. Obviously, the initial conditions chosen here for the drive system and driven system are quite different.

Under the control laws given in Theorems 3, 4 and 6, time histories for the error signals, $e_x(t)$, $e_y(t)$ and $e_z(t)$, obtained for the three cases are displayed in Figs. 7, 8 and 9, respectively. All the three cases show the exponential convergence of the errors to zero, as expected.

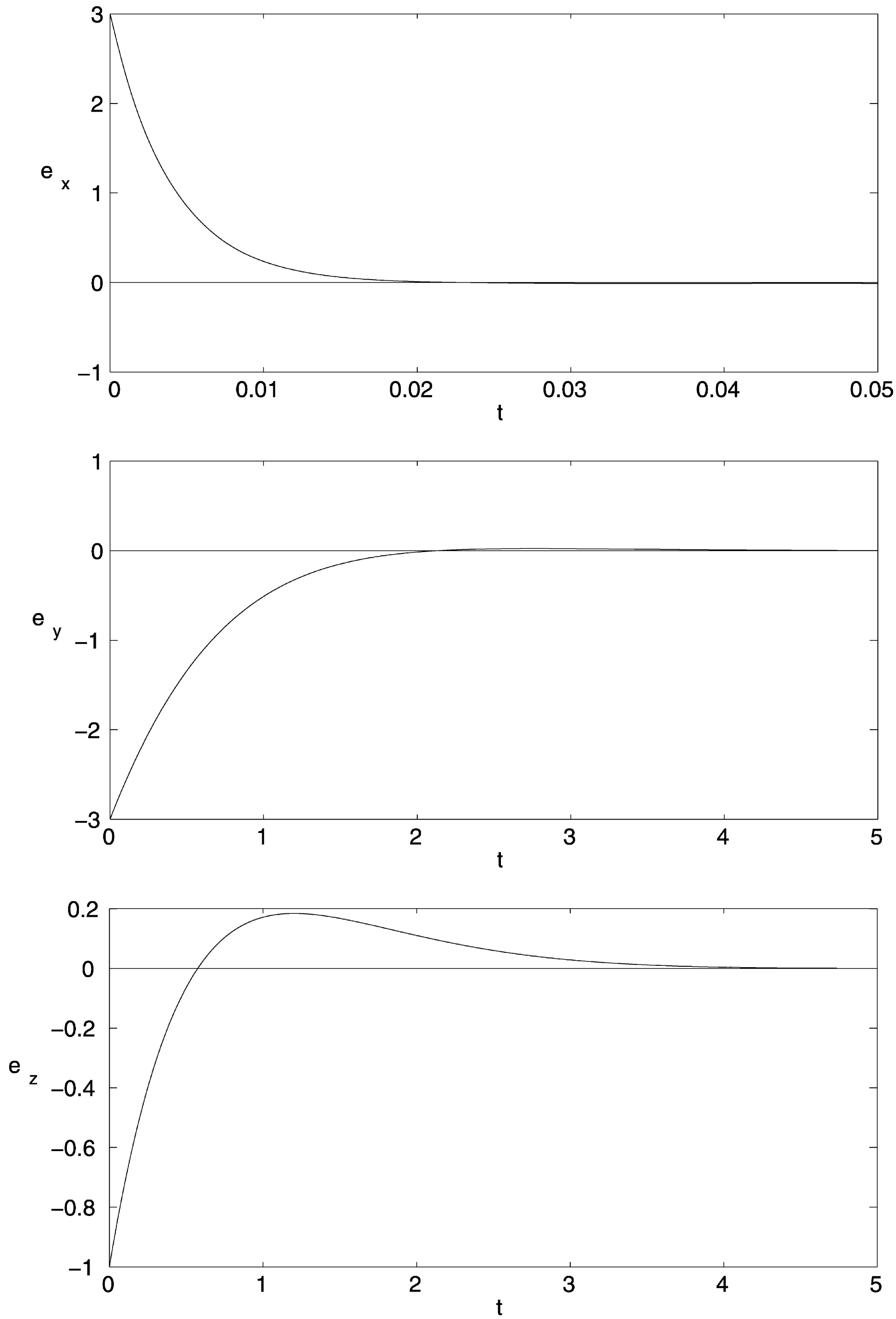

Fig. 7. Time history of error system (17) for $a = b = c = 0.65$, $\tau = 100$, $r = s = 3$ using the control law given in Theorem 3, with the initial conditions, $x_d(0) = 4$, $y_d(0) = 2$, $z_d(0) = 2$ and $x_r(0) = 1$, $y_r(0) = 5$, $z_r(0) = 3$, when $\delta_x = 250$, $\delta_y = 1.8$ and $\delta_z = 0.5$.

For the stabilization problem, we show four examples using the control laws given in Corollaries 1, 3 and 4, and the remaining three cases are similar. The initial conditions chosen for these four cases are respectively given by

$$x(0) = -80, \qquad y(0) = -1, \qquad z(0) = 15, \tag{52}$$

$$x(0) = 0.2, \qquad y(0) = 15, \qquad z(0) = 100, \tag{53}$$

$$x(0) = -20, \qquad y(0) = -1, \qquad z(0) = 5, \tag{54}$$

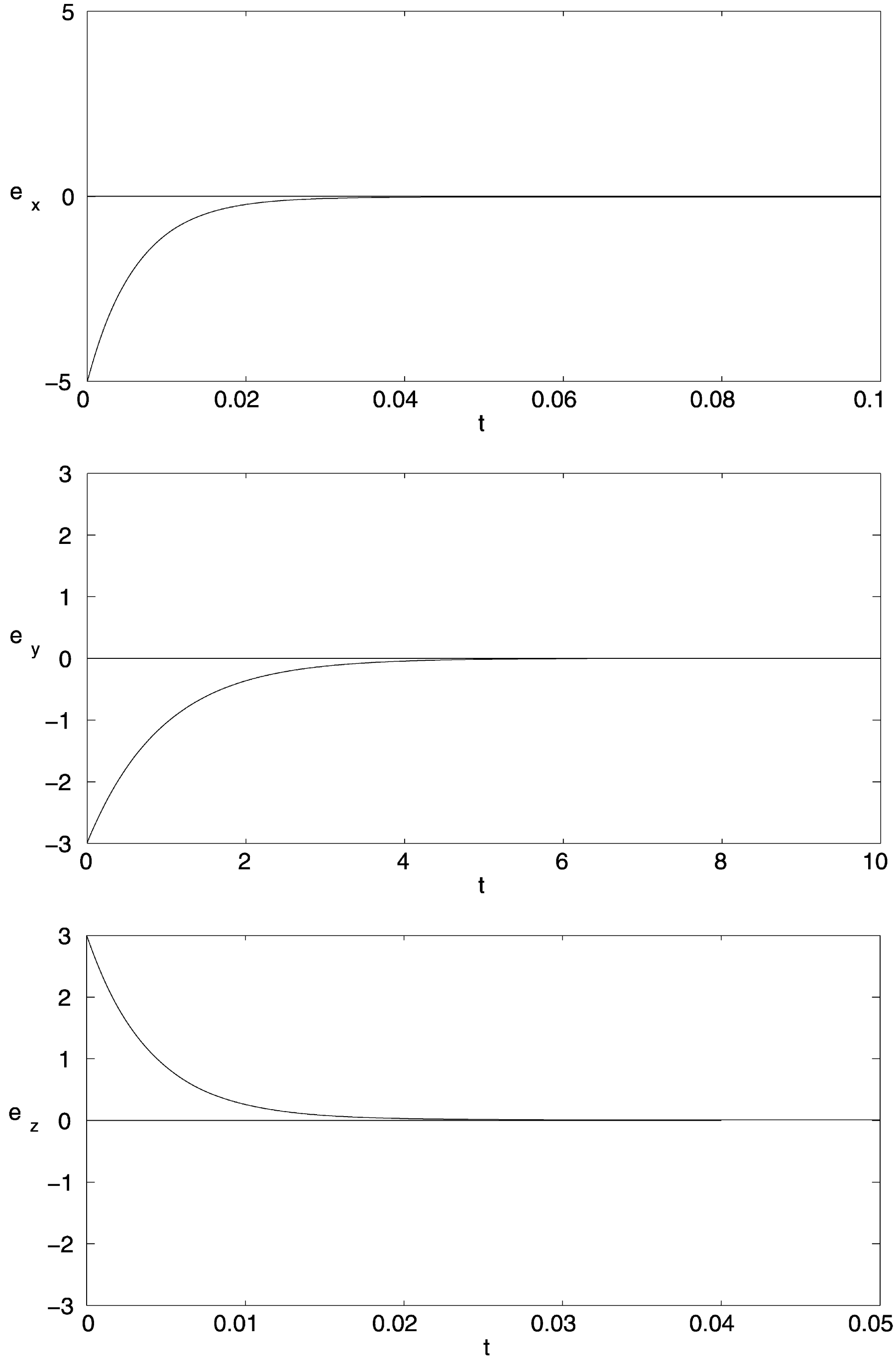

Fig. 8. Time history of error system (33) for $a = b = c = 0.72$, $\tau_1 = \tau_2 = 100$, $r_1 = r_2 = s_1 = s_2 = 1$ using the control law given in Theorem 4(1), with the initial conditions, $x_d(0) = 10$, $y_d(0) = 5$, $z_d(0) = 5$ and $x_r(0) = 15$, $y_r(0) = 8$, $z_r(0) = 2$, when $\delta_x = 160$, $\delta_y = 1.05$ and $\delta_z = 250$.

and

$$x(0) = -0.26, \qquad y(0) = -0.26, \qquad z(0) = -100. \tag{55}$$

When the control law given in Corollary 1 is applied to system (18), using $\delta_x = \delta_y = 1.05$ and $\delta_z = 33.3$, with $E = (0, 0, 0)$ as the designed equilibrium point, it is shown (see Fig. 10(a)) that the trajectory converges to E. Similarly, for the other three cases, numerical simulation results demonstrate that the all solution trajectories converge to the designed equilibrium point with proper control laws applied (see Figs. 10(b) and 11).

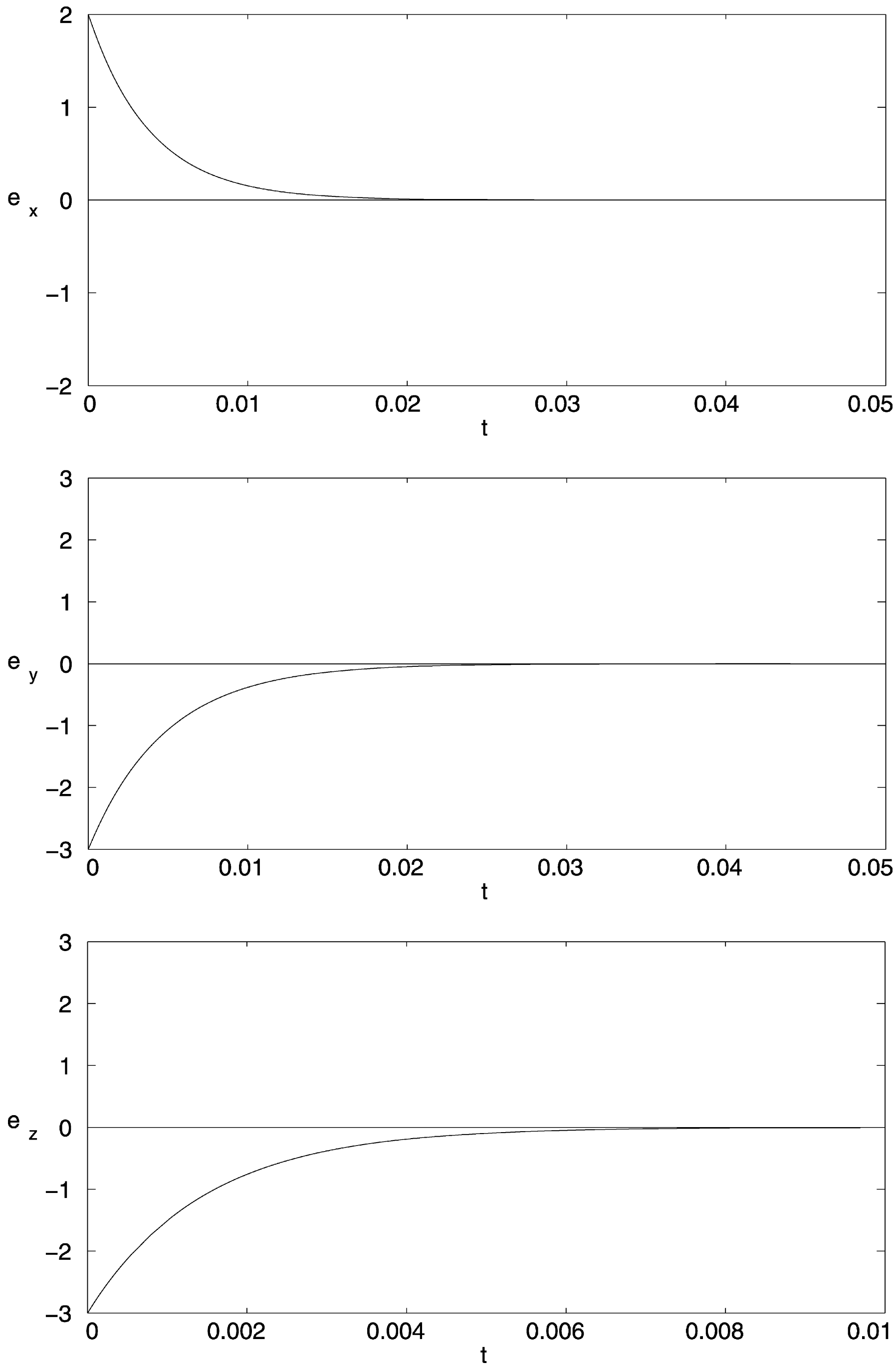

Fig. 9. Time history of error system (41) for $a = b = c = 0.8$, $\tau_1 = 160$, $\tau_2 = 100$, $\tau_3 = 80$, $r_1 = r_2 = s_1 = s_2 = 2$ using the control law given in Theorem 6, with the initial conditions, $x_d(0) = 10$, $y_d(0) = 12$, $z_d(0) = 1$ and $x_r(0) = 8$, $y_r(0) = 15$, $z_r(0) = 4$, when $\delta_x = 255$, $\delta_y = 205$ and $\delta_z = 690$.

10. Conclusion

In this paper, we used hyperbolic tangent function series to develop a method to generate n-, $m \times n$- and $m \times n \times l$-grid-scroll chaotic attractors. Based on the system's equilibrium points and corresponding eigenvalues, simple mathematical analysis is given to identify 1-D, 2-D and 3-D multi-grid-scroll chaotic attractors. For each chaotic system, with the aid of proper chosen Lyapunov functions we designed simple linear feedback control laws to globally exponentially stabilize the system and synchronize two chaotic systems with same structure. Numerical simulation results are presented to confirm the analytical predictions.

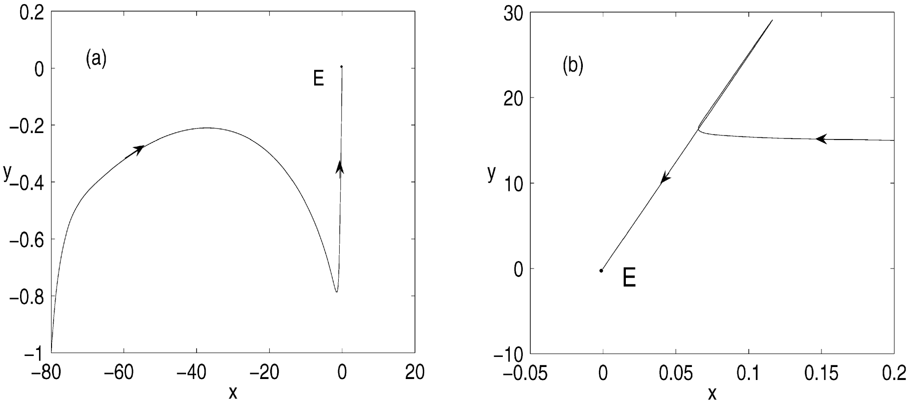

Fig. 10. (a) Trajectory of a double-scroll chaotic attractor for system (18) when $a = b = c = 0.65$, $\tau = 100$, $r = s = 0$ using the control law given in Corollary 1(1) for $\delta_x = \delta_y = 1.05$ and $\delta_z = 33.3$ with the initial condition $x(0) = -80$, $y(0) = -1$, $z(0) = 15$, convergent to the equilibrium point E: $(0, 0, 0)$; (b) trajectory of 1-D-8-scroll chaotic attractor for system (18) when $a = b = c = 0.65$, $\tau = 100$, $r = s = 3$ using the control law given in Corollary 3 for $\delta_x = 250$, $\delta_y = 1.8$ and $\delta_z = 0.5$ with the initial condition $x(0) = 0.2$, $y(0) = 15$, $z(0) = 100$, convergent to the equilibrium point E: $(0, 0, 0)$.

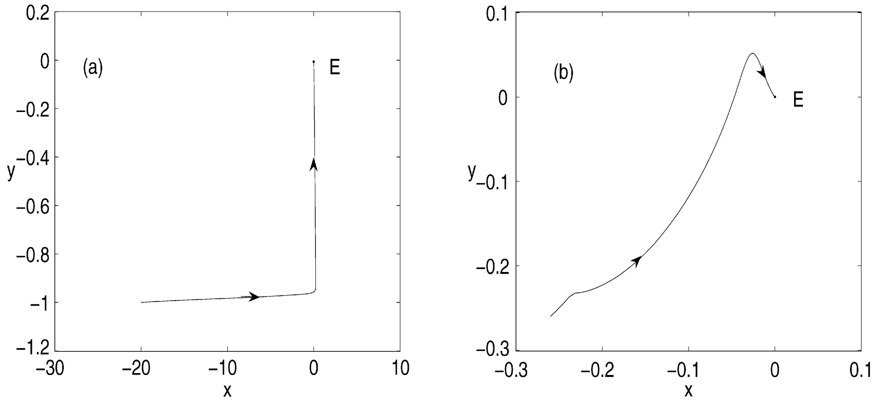

Fig. 11. (a) Trajectory of a 2-D-4 × 4-scroll chaotic attractor for system (37) when $a = b = c = 0.72$, $\tau_1 = \tau_2 = 100$, $r_1 = r_2 = s_1 = s_2 = 1$ using the control law given in Corollary 4(1) for $\delta_x = 160$, $\delta_y = 1.05$ and $\delta_z = 250$ with the initial condition $x(0) = -20$, $y(0) = -1$, $z(0) = 5$, convergent to the equilibrium point E: $(0, 0, 0)$; (b) trajectory of a 3-D-6 × 6 × 6-scroll chaotic attractor for system (45) when $a = b = c = 0.8$, $\tau_1 = 160$, $\tau_2 = 100$, $\tau_3 = 80$, and $r_1 = r_2 = r_3 = s_1 = s_2 = s_3 = 2$ using the control law given in Corollary 6 for $\delta_x = 255$, $\delta_y = 205$ and $\delta_z = 690$ with the initial condition $x(0) = -0.26$, $y(0) = -0.26$, $z(0) = -100$, convergent to the equilibrium point E: $(0, 0, 0)$.

Acknowledgments

This work was supported by the Natural Sciences and Engineering Research Council of Canada (NSERC, No. R2686A02).

References

[1] L. Chua, M. Komuro, T. Matsumoto, The double scroll family, Part I: Rigorous proof of chaos, Circuits Syst. 33 (1986) 1072–1118.
[2] J. Suykens, J. Vandewalle, Quasilinear approach to nonlinear systems and the design of n-double scroll ($n = 1, 2, 3, 4, \ldots$), IEE Circuits Devices Syst. Ser. 138 (5) (1991) 595–603.
[3] F.L. Han, X.H. Yu, Y.Y. Wang, Y. Feng, G.R. Chen, n-Scroll chaotic oscillators by second-order systems and double-hysteresis blocks, Electronics Lett. 39 (23) (2003) 1636–1638.
[4] M.E. Yalcin, J.A.K. Suykens, J. Vandewalle, Experimental confirmation of 3- and 5-scroll attractors from a generalized Chua's circuit, Circuits Syst. I, Fundam. Theory Appl. 47 (3) (2000) 425–429.
[5] S.M. Yu, J.H. Lü, H. Leung, G.R. Chen, N-scroll chaotic attractors from a general jerk circuit, in: Circuits Systems ISCAS, vol. 2, 2005, pp. 1473–1476.
[6] S.M. Yu, J.H. Lü, G.R. Chen, Experimental confirmation of n-scroll hyperchaotic attractors, in: Circuits Systems ISCAS, 2006, pp. 221–224.
[7] M.E. Yalcm, J.A.K. Suykens, J. Vandewalle, Multi-scroll and hypercube attractors from Josephson junctions, in: Circuits Systems ISCAS, 2006, pp. 718–721.
[8] S. Özoğuz, A.S. Elwakil, K.N. Salama, n-Scroll chaos generator using nonlinear transconductor, Electronics Lett. 38 (14) (2002) 685–686.
[9] K.N. Salama, S. Özoğuz, A.S. Elwakil, Generation of n-scroll chaos using nonlinear transconductors, in: Circuits Systems ISCAS, vol. 3, 2003, pp. 176–179.
[10] W.H. Deng, J.H. Lü, Design of multi-directional multi-scroll chaotic attractors based on fractional differential systems, in: Circuits Systems ISCAS, 2007, pp. 217–220.
[11] J.H. Lü, G.R. Chen, X.H. Yu, H. Leung, Design and analysis of multi-scroll chaotic attractors from saturated function series, IEEE Trans. Circuits Syst. I Regul. Pap. 51 (12) (2004) 2476–2490.
[12] J.H. Lü, S. Yu, H. Leung, Design of 3-D multi-scroll chaotic attractors via basic circuits, in: Proceedings of the 4th International DCDIS Conference on Engineering Applications and Computational Algorithms, 2005, pp. 324–328.
[13] E. Ott, G. Grebogi, J.A. Yorke, Controlling chaos, Phys. Rev. Lett. 64 (1990) 1196–1199.

[14] L.M. Pecora, T.L. Carroll, Synchronization in chaotic circuits, Phys. Rev. Lett. 64 (1990) 821–824.
[15] M. Forti, Some extensions of a new method to analyze complete stability of neural networks, IEEE Trans. Neural Networks 13 (5) (2002) 1230–1238.
[16] D. Cafagna, G. Grassi, A new approach to generate hyperchaotic 3D-scroll attractors in a closed chain of Chua's circuits, in: Circuits Systems ISCAS, vol. 3, 2003, pp. 60–63.
[17] D. Cafagna, G. Grassi, New 3-D-scroll attractors in hyperchaotic Chua's circuit forming a ring, Internat. J. Bifur. Chaos 13 (10) (2003) 2889–2903.
[18] P. Yu, X.X. Liao, New estimations for globally attractive and positive invariant set of the family of the Lorenz systems, Internat. J. Bifur. Chaos 16 (11) (2006) 3383–3390.
[19] A. Wolf, J.B. Swift, H.L. Swinney, J.A. Vastano, Determining Lyapunov exponents from a time series, Phys. D 16 (1985) 285–317.
[20] X.X. Liao, Mathematical Theory and Application of Stability, second edition, Central China Normal University Press, Wuhan, 2001.
[21] X.X. Liao, G.R. Chen, On feedback-controlled synchronization of chaotic systems, Internat. J. Systems Sci. 43 (2003) 453–461.
[22] G.R. Chen, Controlling Chaos and Bifurcations in Engineering Systems, CRC Press, Boca Raton, 2000.
[23] G.R. Chen, X.N. Dong, From chaos to order: Perspectives and methodologies in controlling chaotic nonlinear dynamic systems, Internat. J. Bifur. Chaos 3 (1993) 1363–1409.
[24] G.R. Chen, J.H. Lü, Dynamical Analysis, Control and Synchronization of Lorenz Families, Chinese Science Press, Beijing, 2003.
[25] X.X. Liao, Stability Theory and Application of Dynamical Systems, National Defence Press, Beijing, 2002.
[26] X.X. Liao, P. Yu, Analysis on the global exponent synchronization of Chua's circuit using absolute stability theory, Internat. J. Bifur. Chaos 15 (2005) 3687–3881.
[27] X.X. Liao, P. Yu, Chaos control for the family of Rössler systems using feedback controllers, Chaos Solitons Fractals 29 (2006) 91–107.